FATIGUE LIFE OF
DOUBLE NOTCH ALLOY
STEEL BREAKAWAY COUPLINGS

Prepared by:

Illinois Department of Transportation
Bureau of Materials
126 East Ash St.
Springfield IL 62704

July 2022

Technical Report Documentation Page

1. Report No. PRR Number 176	2. Government Accession No.	3. Recipient's Catalog No.
4. Title and Subtitle Fatigue Life of Double Notch Alloy Steel Breakaway Couplings		**5. Report Date** July 2022 **6. Performing Organization Code**
7. Author(s) Christopher Hahin, MetE, CorrE, PE		**8. Performing Organization Report No.**
9. Performing Organization Name and Address Illinois Dept. of Transportation Central Bureau of Materials 126 E. Ash St. Springfield IL 62704		**10. Work Unit No.** **11. Contract or Grant No.**
12. Sponsoring Agency Name and Address Illinois Dept. of Transportation Bureau of Design and Environment 2700 Dirksen Pkwy. Springfield IL 62703		**13. Type of Report and Period Covered** Final Report December 2016-June 2022 **14. Sponsoring Agency Code**
15. Supplementary Notes		

16. Abstract

Double notch alloy steel breakaway couplings have sustained numerous fatigue failures during their service life in Illinois. This report is an in-depth analysis of breakaway couplings that ruptured, resulting in collapse of a light pole falling across a 55-mph expressway. Pole was fortunately cleared away by maintenance before any collisions occurred. This report is an analysis of breakaway coupling stresses derived from peak wind gusts sustained over a 28-year period of service life. The fatigue properties of the couplings made of SAE 4140 steel were also related to their impact and fracture toughness, exposure to deicing salts, and how high wind speed events resulted in fatigue crack propagation. Two recorded wind gusts occurred during service that exceeded 70 mph causing cumulative fatigue damage to the couplings. Couplings were also hot dip galvanized, ostensibly to increase their durability, but were subject to liquid metal embrittlement due to higher tensile strength of air-cooled SAE 4140 steel. Presence of two notches further increases their susceptibility to fatigue failure. Couplings had low impact toughness ranging from 5-6 ft-lbs (7-8 J) at -10° to +60°F (-23° to 16°C). Corrosion-fatigue cracks generated by wind stresses were correlated with propagation rates (da/dN) for structural steels exposed to saline water that formed from dew and deicing salts. Predicted critical crack growth was within 1% of actual crack size at the time of failure. Installation instructions requiring “snug-tightness”, followed by 1/3 turn-of-the-nut, induced a substantial mean stress in the couplings, adding to stresses derived from windstorms. The mean stress was estimated using SAE 4140 data and the Goodman fatigue failure equation. Recommendations are made to change to less susceptible alloys with improved impact toughness and corrosion resistance to deicing salts and salt fall in coastal locations. To prevent future problems, coupling manufacturers must provide specific guarantees to assure a realistic number of years of service life for locations where deicing salts are applied or couplings situated along coastal areas. If failures occur, manufacturer’s cost of replacements, including installation, would be pro-rated based on the guaranteed years of service life.

17. Key Words	18. Distribution Statement
Transportation safety; light poles; double notch breakaway couplings; fatigue; corrosion fatigue; zinc embrittlement	Restricted to Departments of Transportation, Municipal and County Highway Agencies

19. Security Classif. (Of this report)	20. Security Classif. (Of this page)	21. No of Pages	22. Price
Unclassified	Unclassified	60	

Table of Contents

List of Figures

List of Tables

Acknowledgements

The author acknowledges the support of Mr. Mark Seppelt of the Central Bureau of Design and Environment to determine the causes and remedies to this significant safety problem.

The author acknowledges the assistance of Mr. Stan Clow of District 6 in obtaining failed double notch breakaway couplings from various locations in Central Illinois and for pointing out the severity of the problem.

In addition, the author acknowledges the support of the Metals Laboratory of the Central Bureau of Materials in performing machining services, tensile and impact testing of coupling materials, as well as measurement of zinc coating thickness on various couplings.

The chemical composition analysis of Chicago Spectro Services and metallographic work of SGS MSi Laboratories are also acknowledged.

FATIGUE LIFE OF DOUBLE NOTCH ALLOY STEEL BREAKAWAY COUPLINGS

Introduction

Breakaway couplings were initially made of an aluminum alloy with a side-notched spline shape that split apart after long-term service due to intergranular corrosion. The second-generation coupling was a split section that was held together with aluminum rings but sustained corrosion at the interface, causing the coupling to fall apart in service. The manufacturer replaced these previous designs with a double notch alloy steel coupling and coated them with hot-dipped zinc. This report focuses only on double notch alloy steel couplings widely used for light poles in Illinois that are anchored next to highways which could be impacted by vehicles.

On 17 October 2016, a tenon-top light pole fell across Veterans Parkway in Springfield Illinois. Although the pole failed, no accidents or injuries were sustained. The pole was removed from the highway. Highway maintenance personnel stated that there was no evidence that the pole was struck by a vehicle or mower. No dent marks on the pole were observed. The breakaway double notch couplings [Ref. 1] were then removed by maintenance personnel. The coupling fracture surfaces showed the presence of iron oxide, some with a light “flash rust”, indicative of short-term exposure, whereas the other surfaces had presence of darker hematite and effects of burnishing from fatigue cracks opening and closing during stress cycling. This failure was not the first of many other previous failures of double notch breakaway couplings. This report is a comprehensive analysis of why these couplings failed during windstorms. This report does not address failures of breakaway couplings caused by vehicle impacts to light poles. This analysis focuses on one pole that fell over a highway with a 55-mph speed limit. However, this failure analysis is applicable to the service life of double notch couplings of the same design widely used in Illinois and other states.

Based on the fracture surfaces, there was evidence of initial shallow cracking in two couplings, followed by crack advancement and eventual fast fracture and brittle rupture of the remaining couplings. The two couplings with initial deeper cracks and evidence of surface corrosion failed first, whereas the couplings that failed last had larger brittle fast fracture surfaces. The two couplings with larger initial cracks failed first and then transferred their tensile and bending loads to the two remaining couplings. After the remaining two couplings failed, the light pole then collapsed onto the 55 mph expressway.

According to official weather data, the peak wind speed in Springfield on 17 October 2016 was 39 mph during a windstorm that lasted for 16 hours. To understand the causes of the failure, several contributing factors were explored and investigated regarding the design of the couplings, their material properties, and the responses of the light pole to wind forces. These factors included:

a. Stress concentrations associated with the design of the coupling.
b. Coupling material and its manufactured properties.
c. Effects of wind speeds on the light pole and coupling stresses.
d. Effects of galvanizing on fatigue life.
e. AASHTO requirements, including resistance to wind forces.
f. Crack initiation, crack advancement, its relationship to fracture toughness, and ultimate fracture of the couplings.

Coupling Design and Stress Concentrations

1. *Geometry and dimensions*. The double notch alloy steel breakaway coupling [Ref. 1] Is a solid rounded body with an outside diameter of 1.645 ± 0.005” with two deep V-notches. The diameter of the V-notch is 0.675 ± 0.003”. One end has a tapped and threaded hole; the other end has a 2.75” long 1”–8 UNC threaded extension stud. See *Figure 1* for additional dimensions.

2. *Function and characteristics*. The double notch breakaway coupling functions upon impact of the light pole by concentrating both tensile and shear forces into the notched portions. Although the coupling is supposed to fracture at the lower notch which is closest to the anchor bolt, prior pendulum impact qualification tests showed that the upper notch sometimes failed, leaving a residual stub that extends beyond the 4” limitation set by AASHTO. When poles are struck by vehicles, an impact moment is transmitted at the speed of sound that induces stresses in either the lead coupling when in the “diamond” configuration, or two couplings in the “square” configuration (see *Figure 2*). When wind forces are applied either in the “square” or “diamond” configurations, the moments of inertia of the bolting arrangement are the same. Due to the rigid bolted connections with the thick pole base, shear stresses are also transmitted. In “diamond” configuration, two couplings are in the neutral axis, with the force of impact inducing a tensile force on the lead coupling and a compressive force on the trailing coupling. In the “square” configuration, the two forward couplings are subject to tensile forces and the rear couplings are in compression. When the pole vibrates with respect to its fundamental frequency of 1 Hz, this

loading is reversed. Because wind directions are variable, the couplings can experience wind forces in either the “square” or the “diamond” configurations. Depending on wind directions, couplings can also be subject to forces causing reversed bending.

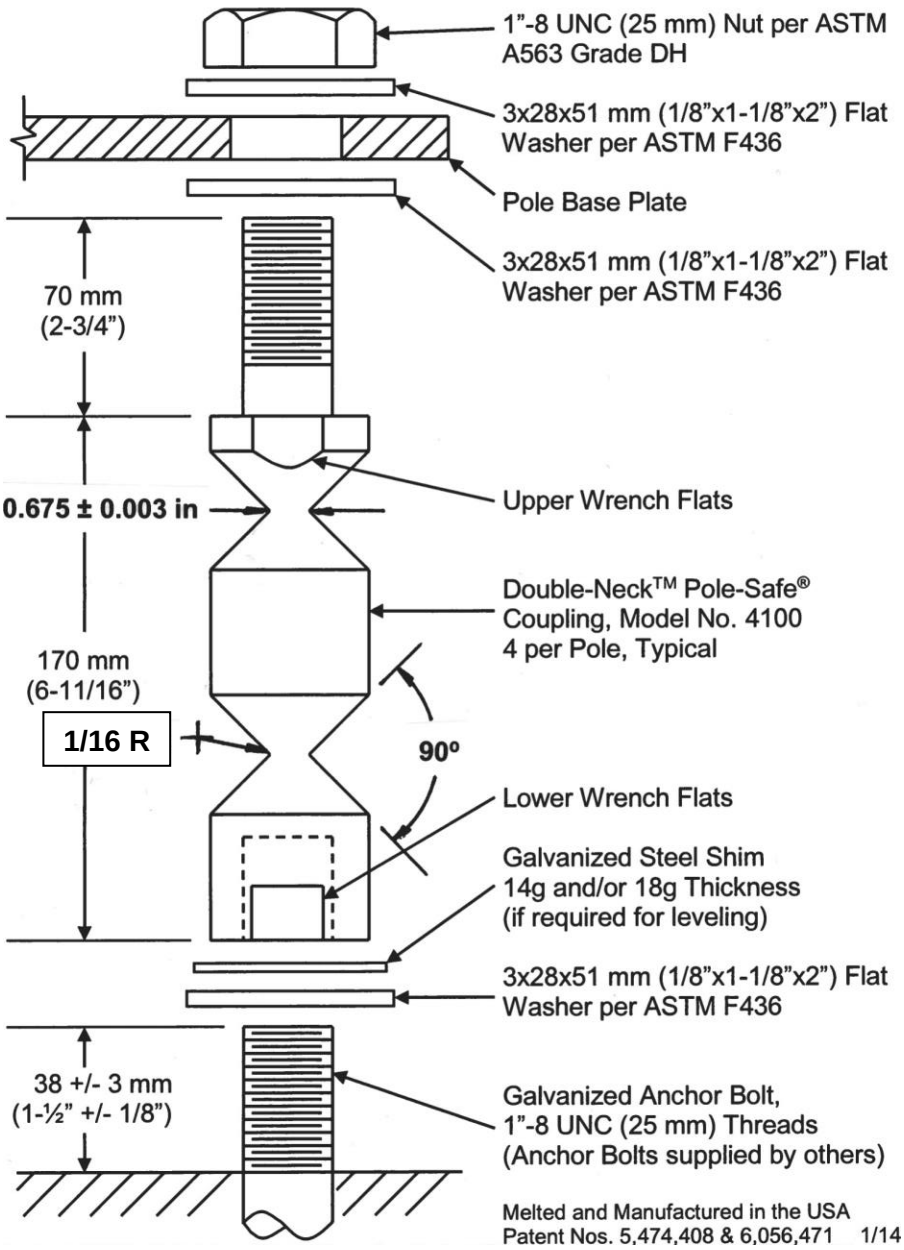

Figure 1. The basic dimensions, shape geometry and fastening components of the double notch coupling, taken from manufacturer installation instructions. The diagram above shows two sharp V-shaped notches, where the radius at each notch is 0.0625 (1/8) in [1.6 mm].

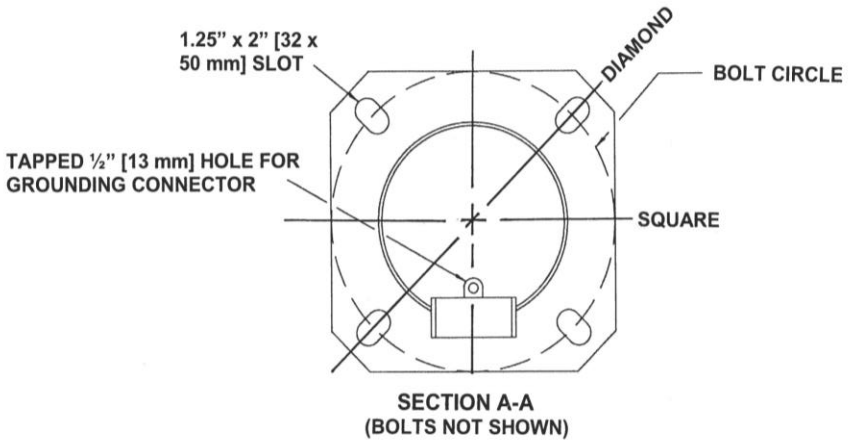

Figure 2. The layout of the pole base plate and how the base is loaded by wind forces that are either perpendicular to the bolt array (square loading) or at a diagonal (diamond loading).

3. *Stress concentrations of the notches.* References in the engineering literature to stress concentrations in round bars with two deep notches is limited. The notch radius of the double notch coupling is 0.0625", the large diameter D is 1.635" and the small diameter d is 0.675", making the r/D ratio = 0.038 ≈ 0.04 and D/d ratio = 2.4. According to [Ref. 2, Noda, Takase and Monda, 1996], this corresponds to a stress concentration factor of $K_t = 3.1$. Although their paper uses an included notch angle of 60°, the difference in K_t between 60° and 90° at this level of notch severity is only 2% [Ref. 3, Peterson, Fig. 38, 1974]. The addition of a second notch does not increase the stress concentration factor according to [Ref. 4, Dragoni and Castagnetti, 2010].

4. Additional verification of stress concentration. The change in area where the anchor bolt is fastened to the coupling is a 1"-8 UNC tapped and threaded hole. This tapped hole section has a net area of $A_{net} = \pi\,(1.635/2)^2 - \pi\,(0.5)^2 = 2.099 - 0.785 = 1.314$ in². The area of the notch is 0.358 in². The ratio of change in area is 1.314 ÷ 0.358 = 3.67. This change in area is in relative agreement with a stress concentration factor range of 3.0-3.7.

Stress concentration in the coupling can also be explained by the changes in moment of inertia from the tapped and threaded hole to fit the anchor bolt in the coupling compared to the moment of inertia of the notched areas. The moment of inertia of the threaded section of the coupling is

$I_{net} = I_{OD} - I_{ID}$. The OD = 1.63" and the threaded hole is 1" in diameter. The moment of inertia of the threaded female portion of the coupling is ($\pi/64 = 0.049$) (1.635^4) – (0.049)(1^4) = 0.301 in^4, whereas $I_{inertia}$ of the notched section is very small ($I = 0.049\ (0.675)^4 = 0.0102\ in^4$.

However, since the couplings are in a 15" diameter bolt circle, moments of inertia substantially increase. For the female threaded connection, its moment of inertia is:

$$I_{thread} = I_0 + AH^2 = 0.301 + 1.314\ (7.5)^2 = 73.9\ in^4.$$

Similarly, the moment of inertia for the notch is:

$$I_{notch} = 0.01 + 0.358\ (7.5)^2 = 20.1.$$

The nominal stress is magnified by the change in moment of inertia by a ratio of 73.9 / 20.1 = 3.68. Although the parallel axis theorem increases the overall moment of inertia of the bolt circle array, the cross-sectional areas of the threaded portion vs. the notch area are the significant terms that account for the difference in their stress levels.

To incorporate the various ranges of stress concentrations encountered in (a) the published technical literature, (b) the presence of two adjacent notches in the coupling, and (c) the sharp changes in moment of inertia, a stress concentration factor of $K_t = 3.1$ was selected in subsequent analyses of the double notch coupling design.

These high concentrations of stress were purposely incorporated into the design of the couplings so that they would easily rupture when poles are impacted by vehicles. Couplings were previously qualified for acceptance by pendulum impact tests that simulated vehicle collisions with a light pole.

Coupling Material and its Manufactured Properties

1. *Composition.* An analysis of the chemical composition of the coupling was performed by Chicago Spectro Service Laboratory in January 2017. The composition was determined by spectrographic analysis as shown in *Table 1*:

***Table 1* / Chemical Composition of the Coupling**

Element	*Double Notch Coupling*	*SAE 4140*
Carbon	0.41%	0.38-0.43
Manganese	0.89	0.75-1.00
Phosphorus	0.013	0.035 max
Sulfur	0.016	0.040 max
Silicon	0.24	0.15-0.35
Nickel	0.11	…
Chromium	0.90	0.80-1.10
Molybdenum	0.23	0.15-0.25
Vanadium	0.17	…
Copper	<0.005	…

NOTE: Where an ellipsis (…) appears, there is no requirement; nickel, vanadium and copper are elements typically reported in the spectrographic analysis of steel.

Although the chemical analysis indicates that this steel could also be either SAE 4142 or 4145, it is most likely SAE 4140 since that alloy is more widely specified and stocked. Also, the carbon content is within the mid-range of SAE 4140. If the alloy is either SAE 4142 or 4145, their impact toughness would be slightly less than SAE 4140 after an air-cooled heat treatment.

2. *Galvanizing*. The coupling was clearly hot dip galvanized. The manufacturer claims in its product specification that galvanizing meets ASTM A653, which is a specification for sheet steel. The appropriate specification for this product is ASTM A123. Based on its nominal diameter, the coupling should have an average zinc coating thickness of 3.4 mils with a minimum of 3.1 mils. Because the couplings have been exposed to the weather for many years, the original zinc coating thickness as it emerged from the galvanizer cannot be verified.

However, there are only a few insolated small areas where the zinc coating is still bright and virtually unoxidized on some couplings. About 95% of the remaining surface areas of the couplings are covered with zinc oxide and other corrosion products of zinc, primarily on the sides of the couplings, where complete penetration of the zinc to the steel substrate in the form of pitting was observed. Rusting of the cracked notch surfaces was evident, indicating inward propagation of surface cracks. The cracked surfaces showed minimal-to-substantial oxidation of the alloy steel, presence of crack initiation sites, fatigue propagation, and final markings of fast fracture rupture. See *Figures 13, 14, 15 and 16* for photographs of the cracked coupling surfaces.

Zinc coating thickness varied substantially in the areas where the zinc coating was still bright. Zinc thickness was measured by a Defelsko Positector 6000 accurate to the nearest 0.5 micron. The zinc thicknesses in locations where limited or virtually no corrosion of zinc was observed are summarized in *Table 2*:

***Table 2* / Thickness of Zinc Coatings Showing Virtually No Oxidation**

Coupling #1		*Coupling #2*		*Coupling #3*	
Zinc Thickness, µm	Zinc Thickness, mils	Zinc Thickness, µm	Zinc Thickness, mils	Zinc Thickness, µm	Zinc Thickness, mils
86.5	3.40	58.5	2.30	91.0	3.58
95.0	3.74	61.5	2.42	78.5	3.09
100.0	3.93	60.5	2.38	71.5	2.81
72.5	2.85	64.0	2.52	80.5	3.16
71.5	2.81	60.5	2.38	96.5	3.80
79.5	3.13	57.0	2.24	83.5	3.29

The mean zinc thickness on surfaces showing virtually no corrosion was 2.99 ± 0.54 mils, indicating that in some locations the zinc thickness was less than the requirements of A123. Based on its location, where salt spray from deicing fluids is present and because couplings are virtually at ground level, the corrosion rate for the zinc coating was estimated at 0.83 mils/year (mpy). See the subsequent section on loss of zinc coating for further description of how this

corrosion rate was determined. Based on a corrosion rate of 0.83 mpy, the time to penetration of 3 mils of zinc is (3 mils) ÷ 0.83 mpy = 3.6 years when exposed to salt spray.

3. *Mechanical properties.* According to the manufacturer's specifications sheet of January 2014 [Ref. 1], the minimum ultimate tensile strength (UTS) is 49.8 kips, and the minimum yield strength (YS) is 43.2 kips. Since the average notch diameter is 0.675", the tensile area is therefore 0.358 in^2. These rated tensile loads indicate that the ultimate tensile strength (UTS) should be 49,800 ÷ 0.358 = 139,160 psi and the yield strength (YS) should be 43,200 ÷ 0.358 = 120,670 psi. Similarly, the ultimate restrained shear strength range varies from 3.8 to 5.5 kips, making the shear strength range 10,614 to 15,363 psi. The ratio of (shear strength) ÷ UTS is therefore 15,363 / 139,160 = 0.11. These ratios are at marked variance with normal ratios for (shear strength) / (UTS) for carbon and alloy steels which typically are 0.75 [Refs. 5, 6]. Mark's Standard Handbook for Mechanical Engineers, 8th Edition, Mc-Graw-Hill, 1978, p 13-18; Machinery's Handbook, 26th Edition, Industrial Press, 2000, p 476.

a. *Hardness tests.* Additional hardness tests were taken on the central core material adjacent to the central notch area. The hardness tests do not bear out the minimum tensile strength ratings as presented by the manufacturer. Hardness values and corresponding tensile strengths were determined from *ASTM A370, Standard Test Methods and Definitions for Testing of Steel Products*. A predictive equation for converting Rockwell B hardness into ultimate tensile strength (UTS) was derived from values in Table 3 and is a polynomial function:

$$UTS = 564 - 12.39 (R_B) + 0.079 (R_B^2)$$

Where UTS = ultimate tensile strength, ksi

RB = Rockwell B hardness number

Based on 19 readings taken from four different couplings, the mean hardness was 102.4 ± 6.4 Rockwell B. Inserting the mean value of 102.4 for Rockwell B into the polynomial function, the UTS obtained was 123.4 ksi. A tensile strength of 123 ksi, according to Table 2 of A370, is approximately equivalent to 26 Rockwell C.

A UTS of 123 ksi is significantly less than the manufacturer rated minimum UTS of 139 ksi. The YS / UTS ratio is virtually constant for SAE 4140. Based on published data for SAE 4140 steel [Ref. 7, American Society for Metals, 1978], the YS for the coupling is approximately 80% of

UTS in the hardness range found in the failed couplings. Based on a UTS of 123.4 ksi for the coupling, the predicted average YS is 98.7 ksi.

b. *Charpy V-notch (CVN) impact tests.* In addition to hardness tests, CVN test specimens were taken from the central core of the couplings adjacent to the central notch. Impact toughness values were very low for each of the four couplings that had failed. The impact energy values were taken at several different temperatures to determine a transition temperature and K_{Id} fracture toughness are summarized in *Table 3*:

***Table 3* / Impact and Fracture Toughness of Coupling Material**

CVN Impact Energy, ft-lbs	*Temperature, ºF*	*Fracture Toughness, ksi [in]* $^{0.5}$
6.0	+60	26.8
5.5	+32	25.7
5.0	+10	24.5
5.5	-10	25.7

The fracture toughness was determined from the CVN test results using the Barsom-Rolfe relationship of [Ref. 8, Barsom and Rolfe, 1987]:

$$K_{Ic} = [4 \times (CVN) \times E]^{0.5}$$

Where K_{Ic} = fracture toughness, ksi $[in]^{0.5}$

CVN = Charpy V-notch energy absorption, ft-lbs

E = modulus of elasticity for steel, 30×10^6 psi

Using the value of CVN = 5.0 ft-lbs, the K_{Id} fracture toughness = 24.5 ksi $[in]^{0.5}$. This value is considered realistic and confirmed by the Roberts-Newton [Ref. 9] equation $K_{Ic} = 9.35\ [CVN]^{0.63}$. When CVN = 5, the lower-bound fracture toughness according to the Roberts-Newton equation is 25.8 ksi $[in]^{0.5}$. Wind speeds at the time of failure exceeded the 16 ft/sec (23 mph) impact speed of a pendulum impact hammer in a CVN test. A K_{Id} value of 24.5 ksi $[in]^{0.5}$ for fracture toughness was therefore used to determine critical crack length and then compared with crack actual depths obtained by metallographic analysis.

A microstructural analysis was conducted to evaluate the condition of the SAE 4140 couplings to gain an insight into their prior thermal processing. This analysis was conducted by SGS MSi, Inc. at its Melrose Park, IL facility. The microstructure at 100x consisted of bainite, acicular ferrite and unresolved pearlite. No tempered martensite was observed or present, which indicated that the SAE 4140 did not undergo rapid cooling to form martensite. Using the US Steel continuous cooling diagram for SAE 4140 steel for a 1.5" diameter bar in *Figure 3* [Ref. 6, p. 125] (Source Book on Industrial Alloy and Engineering Data, ASM, Metals Park, OH, 1978, p 125), it is estimated that the coupling material was subject to relatively slow cooling from austenite (1550ºF is typical) to 50°F for about 500 secs (3º/sec). This also explains why bainite is present. Since no tempered martensite was observed, this accounts for the minimal impact toughness of the couplings.

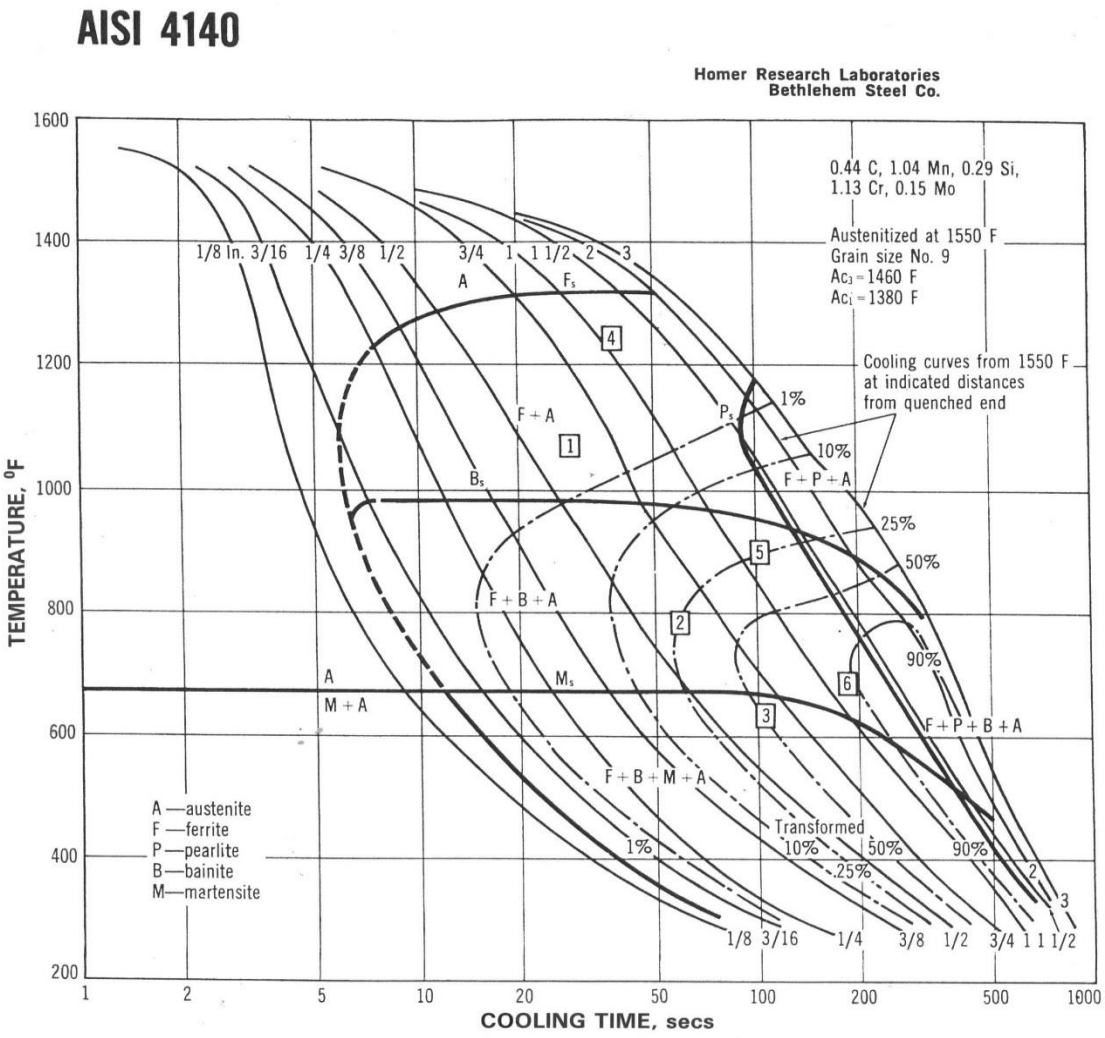

Figure 3. The continuous cooling diagram for SAE 4140 shows that when the cooling rate is sufficiently slow enough, virtually all austenite is transformed into ferrite, bainite, and pearlite. All these phases were present in the microstructure. It is estimated that the CVN impact transition temperature for this coupling is about 54ºC = 129ºF, based on its composition without benefit of quenching and tempering.

Effect of Wind Speeds on Coupling Stresses

1. *General dimensions.* The light pole is 45 ft in height with a tenon to hold the luminaires. The pole diameter at its base is 10” and 4” at the top, with a uniform taper of 0.133 in/ft. At 7 ft height where identification plate is attached, the pole has a 9” mean diameter. See *Table 4* for basic dimensions of the tenon top pole which collapsed.

***Table 4* / Tenon Top Pole Dimensions**

Distance from Base, feet	*Outside Mean Diameter, inches*	*Calculated Area, ft²*	*Remarks*
0.0	10	…	Pole tube welded to base plate here*
7.5	9	11.25	First wind force load area
15	8	…	…
22.5	7	8.75	Second wind force load area
30	6	…	…
37.5	5	6.25	Third wind force load area
45	4	…	Tenon top attached here
47	…	3.0	Two Luminaires and tenon top

The pole base plate is 1.25" thick with a 15" diameter bolt circle and is welded to the tapered tubing. See *Figure 2* for additional base plate dimensions, that are taken from Illinois Highway Standards for tenon top poles.

2. Anchor bolt stresses. Stresses induced by wind forces on the couplings are a function of wind speeds, pole diameters, and the moment of inertia of the anchor bolt geometry. Stress on each coupling depends on the orientation of the anchor bolts with respect to the wind direction. The moment of inertia can be either in the so-called "diamond" direction, where a windward bolt is in tension, two bolts are in the neutral axis, and the leeward bolt is in compression during a wind event. In the "square" orientation, two bolts face in the windward direction, no bolts are in the neutral axis, and two leeward bolts on the opposite side are in compression. These anchor bolt orientations are shown in *Figure 2*. The "diamond" and "square" orientations have specific wind directions, but directions can change frequently during each day, subjecting the couplings to fatigue in both axial tension and rotating bending.

3*. Moment of inertia of notched areas in the "diamond" configuration.* In the "diamond" configuration, two couplings are at the two opposite ends, and two couplings are in the neutral axis. The moment of inertia of the notched area, as defined by a cylinder, is $I = (\pi d^4) \div 64$. The diameter of the notch is 0.675", therefore $I_{notch} = 0.049 \times (0.675)^4 = 0.010\ in^4$. However, due to

the parallel axis theorem $I_{dc} = 2 (I_0 + Ah^2)$, where I_{dc} is the moment of inertia in the diamond configuration, A is the notch section area, and h is the distance from the neutral axis. Since the bolt circle is 15", the distance h = 7.5". Summing up these quantities, the moment of inertia in the diamond configuration is $I_{dc} = 2 (0.01 + 0.358 \times 7.5^2) = 2 (20.15) = 40.3$ in^4.

4. *Moment of inertia of notched areas in the "square" configuration.* In the "square" configuration, four couplings are a set distance away from the neutral axis (see *Figure 2* for the two loading configurations). Since the bolt radius is 7.5", the distance from the neutral axis is $d = \sin 45^o \times 7.5 = 5.303$". There are four bolts around the neutral axis, $I_{sqc} = 4 (I_0 + Ah^2)$, but because h = 5.303", the moment of inertia for four couplings in the square configuration increases to $I_{sqc} = 4 (0.01 + 0.358 \times 28.1) = 40.3$ in^4.

5. Determination of stresses induced by various wind speeds. To determine wind loads resulting from different wind speeds, the 45 ft pole was broken down into three sections, each 15 ft in length. This more accurate method is used to sum up the forces and moments that determine the total moment exerted on the couplings for each wind speed. The mean diameter of each 15 ft section was used to determine the force in lbs/ft^2, because each section is subject to different height and drag coefficients. This method was used to sum up the three moments for the 45 ft pole and the luminaires as described in *Table 5.* The equation to determine the force for the projected area on each pole segment is as follows:

$$P = 0.00256 K_z G V^2 I_r C_d$$

Where

P = pressure, lbs/ft^2

K_z = height factor

G = gust factor = 1.14 (varies up to 1.33)

I_r = importance factor = 1.00

C_d = drag coefficient = $129 \div (C_v Vd)^{1.3}$

C_v = 1.00 for 50-yr recurrence level

V = wind velocity, mph

d = diameter, in feet

6. Height factor. The height factors for light poles based on height and exposure conditions are listed in [Ref. 10, Table 3.8.4-1] in *AASHTO Structural Supports for Highway Signs, Luminaires and Traffic Signals, 6th Edition* (2013). These height factors are plotted in *Figure 4*.

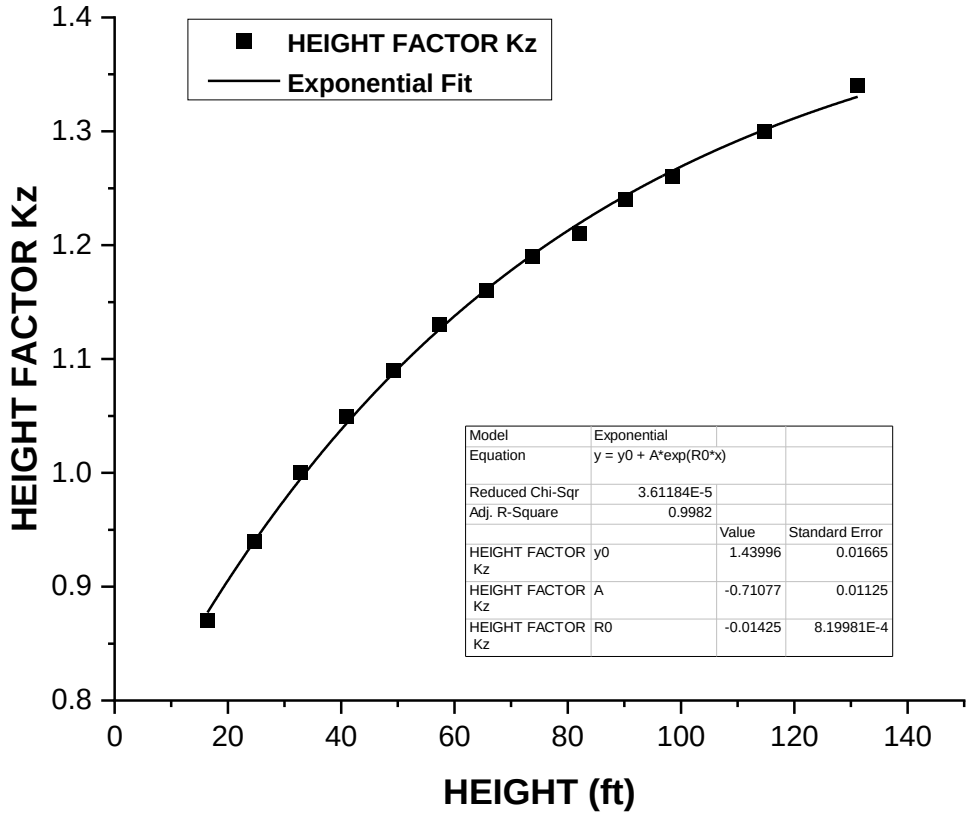

Figure 4. The height factor values were taken from Table 3.8.4-1 in *AASHTO Standard Specifications for Highway Signs, Luminaires and Traffic Signals.* When plotted as a function of height H, the height factor K_z is an exponential function.

The exponential equation that represents the plot of height factor K_z vs. height H in feet was derived from values listed in Table 3.8.4-1, is:

$$K_z = 1.44 - 0.711\, e^{-0.0143\,(H)}$$

For 15 ft, K_z is 0.87; for 35 ft, 1.008; and for 45 ft, 1.07.

7. Area of each segment. The projected frontal area of each 15 ft segment is determined by the relationship A = ½ [a + b] x h, where a is the top of the cone, b is the bottom dimension and h is the height. For the first 15 ft, (a) the frontal area is 11.25 ft^2; for (b) the second segment

(15 to 30 ft), the area is 8.75 ft^2; for (c) the last tapered segment (30 to 45 ft), 6.25 ft^2; for (d) the luminaire segment, has an area of 3.0 ft^2, based on two GE luminaires inclined at 33°.

8. Drag coefficients. Drag coefficients are functions of the wind speed and diameter of the cylinder. Wind drag coefficients C_d were individually determined by use of the formulas and the mph-feet restrictions in [Ref. 6, AASHTO, Table 3.8.6-1].

9. Wind pressures and moments for different wind speeds. Summaries of calculated values for drag coefficients, wind pressures and moments on each 15 ft segment, including luminaires, are plotted in *Figure 5,* and summarized in *Table 5.* The nominal stress is determined by the basic stress equation $\sigma_{nom} = Mc / I$, where M is the moment in in-lbs, c is the distance from the neutral axis (7.5") and I = 40.3 in^4. For concentrated stresses, the nominal stress is multiplied by a concentration factor of $K_t = 3.1$.

The nominal stress in the coupling array is determined by the total moment applied at various wind speeds whereby $\sigma_{nom} = M\ c / I$ = [total moment x 7.5] / 40.3 in^4. The nominal stress was then multiplied by a stress concentration factor of $K_t = 3.1$. Coupling notch stress levels for each wind speed are shown in *Figure 5* or can be calculated from the following polynomial equations for nominal (σ_{nom}) and concentrated (σ_{conc}) stresses, where V is the wind speed in mph:

$$\sigma_{nom} = - 3439 + 198\ V + 1.97\ V^2$$
$$\sigma_{conc} = -10662 + 614\ V + 6.12\ V^2$$

The intercept for the polynomial equation for concentrated stresses has an inherent variance of ± 3.3 ksi.

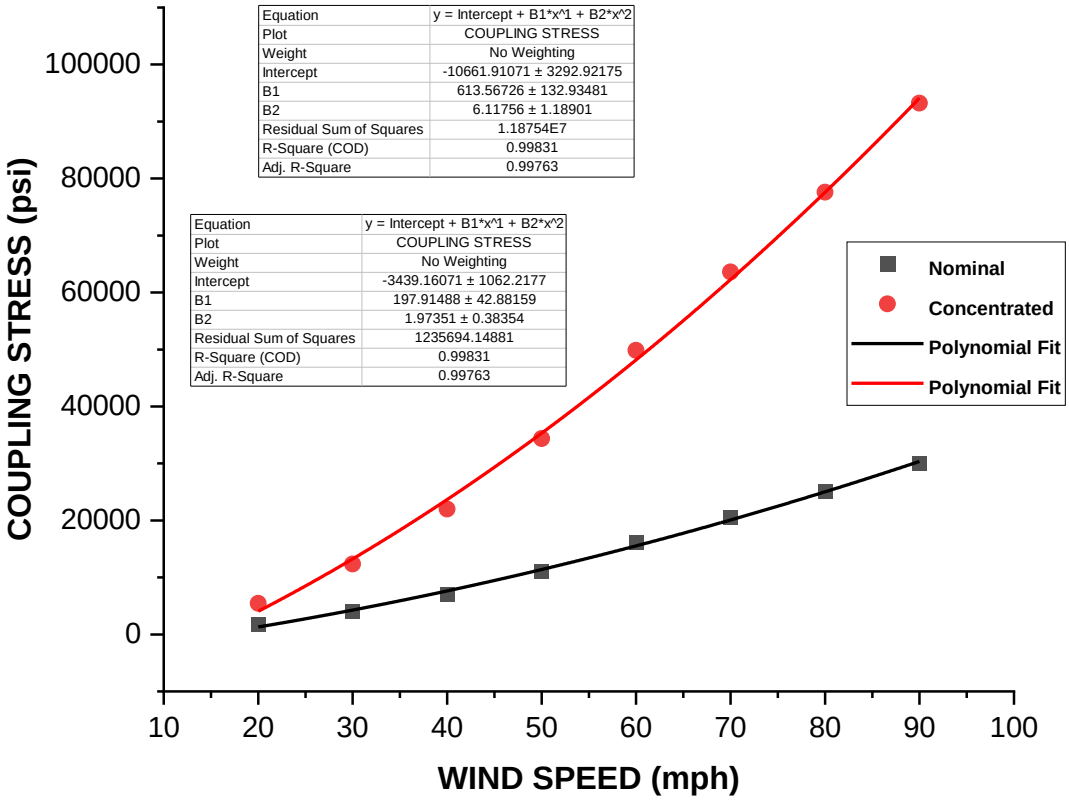

Figure 5. The nominal stress (based on reduced section and moment of inertia only) and concentrated notch stress for each coupling supporting the 45 ft pole are plotted as a function of wind speed. The stress concentration factor for the notch was determined to be 3.1 based on its notch severity and its d/D ratio [Refs. 2, 3].

***Table 5* / Summary of Wind Speed and Stress Parameters**

Wind Speed, mph	Segment, Height, ft	Drag Coefficient [A]	Projected Area, ft^2	Wind Pressure, lbs/ft^2	Moment, in-lbs	Nominal Stress, psi	Notch Stress, psi [B]
20	15	1.10	11.25	1.12	1134		
	30	1.10	8.75	1.26	2986		
	45	1.10	6.25	1.37	3864		
	Luminaire	0.70	3.00	0.82	1387		
				Total Moment	9371	1744	5406
30	15	1.10	11.25	2.51	2545		
	30	1.10	8.75	2.83	6880		
	45	1.10	6.25	3.09	8695		
	Luminaire	0.70	3.00	1.96	3316		
				Total Moment	21436	3989	12366
40	15	1.10	11.25	4.47	4525		
	30	1.10	8.75	5.03	12238		
	45	1.10	6.25	5.50	15469		
	Luminaire	0.70	3.00	3.48	5895		
				Total Moment	38127	7096	22000
50	15	1.10	11.25	6.98	7069		
	30	1.10	8.75	7.55	19111		
	45	1.10	6.25	8.25	24159		
	Luminaire	0.70	3.00	5.44	9212		
				Total Moment	59551	11082	34354
60	15	0.91	11.25	8.32	10179		
	30	1.10	8.75	11.33	27519		
	45	1.10	6.25	12.37	35438		
	Luminaire	0.70	3.00	7.84	13265		
				Total Moment	86401	16080	49848
70	15	0.75	11.25	9.33	9447		
	30	1.04	8.75	14.57	35414		
	45	1.10	6.25	16.83	47334		
	Luminaire	0.70	3.00	10.67	18054		
				Total Moment	110249	20518	63606
80	15	0.63	11.25	10.24	10368		
	30	0.87	8.75	15.92	38698		

	45	1.10	6.25	21.98	61819		
	Luminaire	0.70	3.00	13.94	23586		
				Total Moment	134471	25026	77581
90	15	0.54	11.25	11.25	11249		
	30	0.75	8.75	17.37	42218		
	45	1.10	6.25	25.48	78244		
	Luminaire	0.70	3.00	17.64	29847		
				Total Moment	161885	30067	93207

A The drag coefficient for the luminaires is based on a projected area of 3.0 ft^2 derived from luminaires inclined at 33°, resulting in a C_d = 1.28 sin 33° = 0.697 ≈ 0.70. Other drag coefficients are for round cylinders at different diameters and wind velocities.
B The notch stress incorporates a stress concentration factor of K_t = 3.1.

On the day of the pole failure, the peak wind gust speed was 39 mph. The concentrated stress at the coupling notch was calculated at 22.6 ksi, based on gust factor of 1.14. The CVN impact toughness of the coupling core metal was 5 ft-lbs. The equivalent K_{Id} fracture toughness was determined by the Barsom-Rolfe equation $K_{Id} = [4 \times CVN \times E]^{0.5}$ where E = 30 x10^6 psi for steel [Ref. 8]. The K_{Id} value for fracture toughness per this equation is 24.5 ksi [in]$^{0.5}$**.**

The fracture mechanics compliance K_I for a notched round bar has been defined in [Ref. 11]. However, this compliance method to determine K_I is based on a uniform circular pre-crack all around the notch. See the Appendix of this report for fracture toughness of a round bar with a sharp central notch similar to the double notch breakaway coupling analyzed in this report, except that the compliance specimen has a uniform peripheral notch crack.

The fractured breakaway couplings in this report show substantial surface corrosion from pre-cracked and crack advancement areas, but the cracks are predominantly on one side of the coupling, as shown in photographs in a subsequent section of this report. Because of this, compliance K_I was taken from a crack on one side of a plate in tension. The crack depths in the couplings varied from 0.051” to 0.191”. The couplings along Veterans Parkway were apparently oriented in the “square configuration” with respect to roadway placement. However, one of the couplings does not show sizable pre-cracked areas. This appears to indicate that two couplings failed first and two others were primarily in the neutral axis. Moreover, predominant high wind events were coming from the southwest or southern directions. Since each coupling contains

two notches, the precise order of notch failures on the remaining two couplings cannot be determined at this time. The remaining couplings sustained load transfers, as evidenced by their fracture surfaces and flash rust, indicating limited exposure to atmospheric moisture.

AASHTO Materials and Wind Load Requirements

1. *Material requirements.* Based on construction records, the poles on this section of Veterans Parkway (Illinois 4) were apparently installed in 1987. The applicable AASHTO code standard at the time of installation that governed vertical supports for light poles was *Standard Specifications for Structural Supports for Highway Signs, Luminaires and Traffic Signals,* which included interim specifications of 1986-1989 from the AASHTO Subcommittee on Bridges and Structures. These requirements have since been modified in the revised LRFD code first published in 2013. Although breakaway couplings provide direct vertical support to light poles, they are also considered as frangible in certain circumstances if warranted by the owner where there is a strong possibility of being horizontally struck by vehicles errantly leaving the highway. Although a distinction is made between a structural and a breakaway structural support, the AASHTO specification at the time of installation in 1988 stated that in Section 1.2.5 (4) that "The vertical supports for luminaire structures…shall be designed for the effects of wind from any direction." Breakaway couplings are placed in vertical positions and structurally support the light pole. In this report, breakaway couplings are considered as vertical structural supports of light poles, in addition to their frangible characteristics.

a. *Impact energy.* At the time of construction, according to AASHTO requirements in Section 4.1.4.1 Allowable Stresses, subsection (3) states that "All steels greater than ½ inch in thickness used for structural supports for highway signs, luminaires and traffic signals that are main load carrying tension members shall meet the current AASHTO specifications for notch toughness requirements." The section diameter of the double notch coupling is 0.675". For the coupling to meet the AASHTO requirement of 25 ft-lbs at -30°F the SAE 4140 would be required to be quenched & tempered. There are no AASHTO impact toughness material requirements for breakaway supports in Section 7, except that they must fracture at certain impact speed ranges of colliding vehicles so that changes in deceleration do not exceed a specific rate. The impact speed of the pendulum hammer when it impacts a Charpy V-notch specimen is 16 ft/sec (23 mph), typically less than the speeds of actual vehicles striking light poles. Breakaway supports, which need to fracture immediately, were apparently exempted from requirements of Section 4.1.4.1, although this was not directly stated in the AASHTO specification in effect at the time of installation.

b. *Wind speed requirements*. According to Section 1.2.4 of the AASHTO code in effect at the time of installation, the 50 year mean recurrence wind maps were to be used for luminaire support structures that exceed 50 ft. Since the pole is only 45 ft in height, the 25 year mean recurrence map of Fig. 1.2.4B was required. For Springfield IL, 70 mph is the wind speed load that was to be applied for design purposes. Moreover, the 25 year mean recurrence interval of Fig. 1.2.4B shows that the 70-mph line is on the outskirts of Springfield, whereas the 50 mean recurrence interval map of Fig. 1.2.4 includes all of Springfield. This small difference shows that within the arbitrary cut-off of 25 years, Springfield would be in the 80-mph zone after 25 years. However, the requirement of 70 mph is not absolute considering that wind speeds vary from one location to another over distances of less than one mile. The pole was in service for 28 years minimum, ostensibly extending it into the 50 year mean occurrence interval. The poles, nor the breakaway couplings, do not carry any guarantee of life span, nor does Section 7 Breakaway Supports of [Ref. 10, AASHTO] require any life span, except for performance or termination of use after vehicle impact.

During the life span of this pole, two wind events occurred when wind speeds at the Springfield airport were recorded at 71 mph (16 August 1987) and 74 mph (19 April 2002). According to Google Earth Pro, the Springfield Airport is 2.4 miles distant from the location where the pole failed, where wind speeds could have been slightly less than 70 mph. Considering the average and arbitrary nature of the of the AASHTO wind speed map, minor excursions of 1 to 3 mph over the 70 mph design criteria are not significant. Gust factors for winds were 14% to 33% more than nominal non-gusted wind speeds and are considered in the wind pressure formula. Variations of 71 to 74 mph is only 1.4 to 5.7% over the 70 mph design criteria and is within a 33% gust factor allowance.

2. Fatigue life requirements. According to Section 11 of *AASHTO Structural Supports for Highway Signs, Luminaires and Traffic Signals* (1986-1994), there are no specific fatigue requirements designated for breakaway couplings. However, Section 12.6 of the present AASHTO LRFD code (6th Edition) states that the durability requirements for breakaway couplings "…shall meet the durability requirements for the material that is used in the steel, aluminum, wood, and fiber-reinforced plastic design sections, as applicable." The durability requirements of the present code for materials chosen for breakaway coupling components do not apply since it was not in effect at the time of installation. Moreover, fracture characteristics of breakaway couplings for safe vehicle collisions with poles do not necessarily coincide with the

fracture toughness of the other pole components, such as base plates, bolting, tapered steel or aluminum alloy tubing, and weldments.

3. *Material properties and relationship to fatigue life.* A realistic approach in this report was taken and considered the fatigue characteristics of galvanized SAE 4140 steel when this alloy was subject to moist or salt spray conditions, also taking stress concentrations into account and wind load ranges up to the 70-mph requirement.

The couplings in question had an average tensile strength of 123 ksi. High cycle fatigue strength is often called the "endurance limit" in the older technical literature. The high cycle fatigue strength for SAE steels of 4130, 4140 and 4340 series with similar tensile strengths have been previously determined [Ref. 12, Grover, Gordon and Jackson, 1960] by testing of round smooth specimens with and without notches and stress-cycled in rotating bending (similar to the double notch coupling). The effect of a 90º V-notches and galvanizing on the fatigue strength of SAE 4140 with a tensile strength 123 ksi is shown in *Table 6.*

An SAE 4140 smooth machined round bar (not galvanized), when its tensile strength is 123 ksi and fatigued in reversed bending, is estimated to have a high cycle (107) fatigue strength range in dry air of 61.5 to 67.5 ksi, based on known fatigue ratios of 0.50 to 0.55. A fatigue strength of 66 ksi was selected from [Ref. 12] and adjusted for the decrease in UTS to 123 ksi.

As shown in *Table 6,* a notch on a SAE 4140 bar with a stress concentration factor K_t of 3.1 substantially reduced its fatigue life. The high cycle (10^7) fatigue strength for SAE 4140 at a stress concentration of 3.1 and 123 ksi tensile strength at cycles is only 23 ksi.

Other tests on the fatigue life of SAE 4140 at different tensile strengths and on other similar steels confirm the detrimental effects of notches. The notches in the fatigue tests described in [Ref. 12] ranged from unnotched to $K_t = 5.0$. Effects of notch severity are shown in *Figure A1*. At higher tensile strengths above 170 ksi for SAE 4140 steel, high cycle fatigue strength is parabolic and no longer follows a purely linear behavior when correlated with tensile strength, as shown in *Figure 6*. The coupling had a tensile strength of 123 ksi based on its Rockwell hardness. Since the tensile strength S_U is 123 ksi, high cycle fatigue strength for an SAE 4140 smooth polished round bar was estimated to be 66 ksi.

4. *Fatigue life and effects of galvanizing.* As early as 1932 [Ref. 13, Swanger and France, April 1932] it was established that galvanizing reduced the high cycle fatigue strength of steels. See Appendix *Figure A5* for the empirical equation to determine the loss of unnotched fatigue strength in dry air by galvanizing the steel. This reduction of fatigue strength has been re-verified by subsequent studies in both rotating bending and axial load testing.

Although the mechanisms were not fully understood in 1932, more recent studies have established that the galvanizing bath and the intermetallic layers of the zinc coatings can act as surface crack initiators which reduce fatigue life [Ref. 14, Okafor, O'Malley, Prayakarao and Aglan, 2013]. Because all steels have surface irregularities, such as grain boundaries, inclusions, surface imperfections caused by hot rolling, machining, or the presence of oxide delaminations, they are sources for intrusion of the brittle intermetallic layers of the zinc coating.

These zinc layers are designated as eta (pure zinc); zeta (6% iron); delta (7-11.5% iron) and gamma (20.5-28% iron) [Ref. 15, US Steel, 1971]. The gamma layer of zinc is located at the steel interface and is the most brittle layer. Zinc bath additions of bismuth, tin, lead are considered wetting agents due to their low melting points but tend to enhance liquid metal embrittlement [Ref. 16]. (M. Vermeersh, W. De Waele, N. Van Caenegem, LME Susceptibility of Galvanized Welded Structures of High Strength Steels, *Sustainable Const & Design,* 2011, 442-447). The brittle gamma interface layer provides crack sites in the steel substrate that reduce the crack initiation time to crack propagation during cyclic fatigue.

Prior to galvanizing, the double notch coupling was machined. The surface finish of the coupling body was estimated to be within a range of 125-250 µin, although notches appeared to have a surface roughness of about 64 µin. For a component with a UTS of 123 ksi, fatigue strength reduction with a surface finish of 250 µin is about 0.75 to 0.80. Since the coupling notches are relatively smooth, a long-term fatigue strength of 66 ksi was assigned. However, because the coupling has a severe stress concentration at the notches, its high cycle fatigue strength at 10^7 cycles was decreased to 23 ksi.

In the "square" configuration against the wind, couplings are in alternating axial tension and compression. In the "diamond" configuration, depending on wind directions, the couplings in the approximately neutral axis are in a minimal loading condition simulated by reversed bending.

However, when wind directions change, the couplings in the formerly neutral axis can then be placed in primary tension or a combination of rotating bending and axial tension.

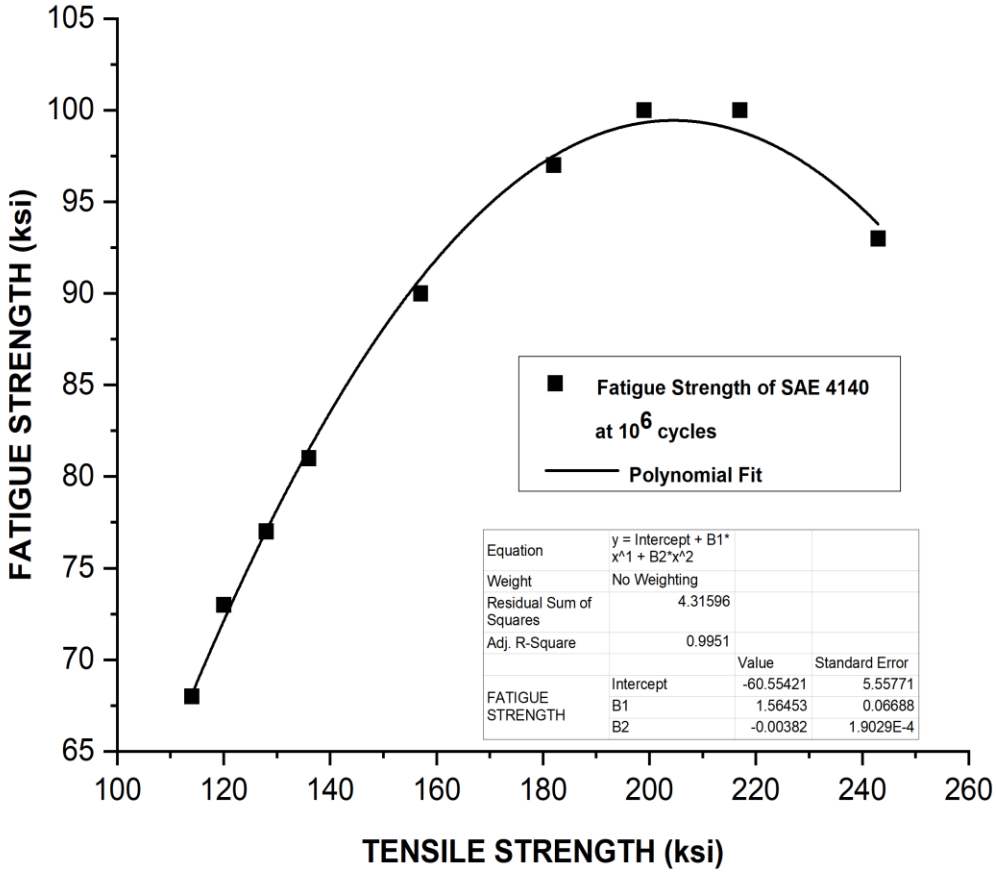

Figure 6. The fatigue strength of 0.40% carbon alloy steels vs. tensile strength is linear when 160 ksi or less, but forms a parabolic peak from 180 to 220 ksi. The polynomial function for several alloy steels fatigue strength vs. tensile strength is $S_f = -60.6 + 1.56\ (S_u) - 0.00382\ (S_u)^2$, where S_f is fatigue strength and S_u is tensile strength at 10^6 cycles, both in ksi. The intercept variance of this equation is ± 5.6 ksi, which accounts for the difference in fatigue strengths of various alloy steels.

With a fatigue strength of 39 ksi at 10^5 cycles, a notched breakaway coupling could withstand a windstorm of 60 mph at most, based on nominal unconcentrated stress values obtained from *Figure 6*. At 70 mph, the nominal stress reached in the coupling was 34.4 ksi, greater than the

estimated fatigue strength of 24 ksi for notched SAE 4140 at 10^6 to 10^7 cycles in reversed bending. When a stress concentration factor of 3.1 is included, stress increases to 107 ksi, which approaches the 123 ksi tensile strength of the coupling.

***Table 6* / Fatigue Life Cycles of Notched*, Unnotched and Galvanized SAE 4140 Bars and Couplings at Various Stresses, ksi**

Fatigue Strength in Various Loading Conditions	*Number of Cycles to Failure*						
	10^4	4 x 10^4	10^5	4 x 10^5	10^6	4 x 10^6	10^7
Unnotched 4140 in Reversed Bending, ksi [A]	99	88	81	70	66	66	66
Notched Coupling, K_t at 3.1, not Galvanized, Reversed Bending, ksi [B]	55	47	39	30	24	24	23
Unnotched 4140, Galvanized, Reversed Bending, ksi [C]	…	78	62	40	38	38	38
Notched Coupling, K_t at 3.1, Zinc Depleted, Reversed Bending, in Saline Media, ksi [D]	51	44	30	25	19	15	12

**NOTES:* [A] Unnotched bar in [Ref. 12, Grover, et. al.] was taken from 0.40% carbon Cr-Mo-Ni alloy steel, quenched in oil from 1550ºF and tempered at 1200ºF, with a UTS = 127 ksi and fatigued in reversed bending. [B] Effect of notch severity of K_t of 3.1 was obtained from fatigue data of a 4130 Cr-Mo alloy steel of similar composition with a 117 UTS and 99 ksi YS, with K_t ranging from 1.5 to 5, taken from [Ref. 12]. [C] Galvanizing fatigue reduction factors were taken from fatigue data of [Ref. 13, Swanger and France] of a 0.45% carbon steel with a tensile strength of 122 ksi. [D] After 4 years, it was estimated that the effects of galvanized brittle zinc-iron coatings were largely dissipated but afforded little-to-no protection from corrosion fatigue, based on data from [Ref. 17, Slunder and Boyd, 1983] which became the predominant source of fatigue cracking after long-term service.

The fatigue strengths in saline media in *Table 6* are for continuous immersion, which would apply to conditions of frequent applications of deicing fluids, or continuous salt fall or ocean spray in coastal locations based on fatigue reductions obtained from corrosion fatigue of SAE 4140 [Ref. 27, Lee and Uhlig]. A notch with a stress concentration of $K_t = 3.1$ has a greater effect on fatigue than galvanizing. However, since the fatigue life of a galvanized coupling was not tested, this report does not speculate as to effects of galvanizing on the notch, but certainly the notch severity provides sufficient opportunity for cracks to start in the brittle zinc-iron delta and gamma coating layers. The number of cycles to failure for SAE 4140 in saline media were for continuous immersion at constant temperature. When couplings are in locations where

average temperatures are significantly less than 20°C and have only intermittent exposures to saline media, the number of cycles to failure will significantly increase.

However, the limited notch toughness of the SAE 4140 coupling and any breaches in the zinc coating can create shallow microcracks. If the zinc coating is depleted, moisture can create pits or dissolution of SAE 4140 base metal. Other than the peripheral crack initiation sites in the notch, there was limited penetration of the zinc coating in the remaining areas without cracking being present. Cracking in only a limited section of about 120° along the notch root was noted in many other failed couplings.

Most of these hairline cracks were not visible before rupture when the couplings were either wetted during rainstorms or from condensation when the relative humidity was sufficient to form dew. No rust bleed-out at cracks was noted due to their tightness and the presence of (a) obscuring corrosion products of zinc in the form of oxides and carbonates, (b) the limited galvanic action of the zinc coating, and (c) the natural bluish-white color of zinc itself. Although the zinc was not chemically analyzed, when copper is present in the zinc, a bluish color results after exposure to the atmosphere.

5. *Effects of moisture, salt, and notches on fatigue life.* Exposure to moisture or salt spray can further decrease the fatigue strength of exposed steel even more to about 40% of its high cycle fatigue strength. The greater the severity of the notch stress concentration also affects fatigue life. The fatigue life of steels in dry air is linearly related to fatigue life up to a tensile strength of 160 ksi . When moisture results from condensation of water vapor in the air, or if the steel has fluids applied or form solutions containing chlorides or sulfides from dew, this can eliminate the linearity with tensile strength when fatigued in dry air. Also, corrosion fatigue strengths decrease as the tensile strength of the alloy increases, as shown in *Figure 8.* With the presence of corrosion pits, the high cycle fatigue strength of SAE 4140 could be reduced from 36.6 ksi after galvanizing to as low as 12-15 ksi when subjected to salt spray after the zinc coating is depleted. At 39 mph, a common wind speed occurrence in Illinois, the calculated nominal coupling notch stress was determined to be 7.3 ksi and 22.6 ksi due to stress concentrations derived from its hourglass V-notch shape.

6. *Loss of zinc coating.* There are several areas on the galvanized coatings where loss of zinc resulted in penetration into the steel substrate (see *Figures 7 and 12-15* for photos). Two couplings had sustained a considerable loss of zinc, as shown by surface roughening and the formation of zinc oxide which covers more than 80% of its surface. According to the Model 4100 information sheet, the couplings were galvanized in accordance with ASTM A653. Specifying this standard makes no sense because A653 is for sheet products. The correct standard for bar products is ASTM A123. If A123 was specified, based on the size of the coupling, typical zinc thickness would range from 3.0 to 3.9 mils. The average zinc thickness on the recovered couplings was 2.99 mils on virtually uncorroded areas, which indicates that the couplings probably would have met the requirements of A123.

Veterans Parkway of Illinois 4 has a suburban atmosphere. However, the couplings are at ground level where they are subject to salt-spray during the winter and moisture condensation during the spring, fall and summer, along with pickup of debris. The long-term corrosion rate for zinc for hardware and structural shapes in atmospheric environments where the zinc is well-drained and dried is 0.097 to 0.104 mils/year, but if subject to salt spray or salt fall the corrosion rate increases to [Ref. 17, p. 106]. If the zinc coating(Zinc its Corr resistance, p106. When zinc is coupled to an alloy steel, its corrosion rate is elevated considerably [Ref. 17, p. 151]. More recent studies of pure zinc in mild saline solutions showed that within 14 days, zinc sustains a corrosion rate of 2.5 mpy [Ref. 18] Y. Meng, et al, Initial Formation of Corrosion Products on Pure Zinc in Saline Solution, Bioactive Materials, Vol 4., Dec 2019, pp 87-96. Since the zinc is constantly picking up moisture by condensation and near ground level where dust collects, the corrosion rate is 2.5 mils/year (mpy) upon initial exposure. To adjust to temperature effects in Illinois from 20°C to 10°C, this rate is reduced by a factor of 0.532, making the initial corrosion rate 1.33 mpy. For a coating thickness of 0.003” (3 mils), assuming complete uniformity of penetration and coating thickness, the galvanized zinc coating would be penetrated in 3.6 years turning to zinc oxides and chlorides. After receiving salt spray, a 3-mil zinc coating would be depleted in about 3 years in some sections of the coupling. The bottom sections sustained the largest losses of zinc coating. Due to formation of protective corrosion products, corrosion rates are substantially reduced to 0.2-0.3 mpy, whereby the zinc coating will be intact after 15 years. This of course assumes that the corrosion penetration rate is completely uniform. However, pits developed (they are black in color), which indicates penetration into the steel substrate. Typical surface conditions after exposures to conditions after 28 years are shown in *Figure 7*.

Figure 7. The zinc coatings on the couplings had degraded by forming zinc oxides and chlorides (oxides are white and yellow; chlorides are white) as a function of long-term exposure to moisture, salt spray and the accumulation of dirt and debris. Note the formation of pits in the sides of the couplings when the zinc coating was depleted. Pits also formed at notches, leading eventually to deeper cracks.

7. *Corrosion fatigue, pit formation, and crack growth rates*. The crack propagation and fatigue strengths of 4140 and 4340 and 4130 steels are similar and directly related to their tensile strengths when fatigued in dry air. However, increasing tensile strength of steels does not translate to a proportional increase in fatigue strength as in dry air when exposed to saline solutions. The presence of chlorides substantially decreases fatigue strength in carbon and alloy steels to as low as 10-14 ksi in 3% NaCl, as shown in *Figure 8.* (taken from [Ref. 19]). C. Jaske, J. Payer and V. Balint, *Corrosion Fatigue of Metals in Marine Environments,* Defense Metals Information Center Report MCIC, Columbus, July 1981, p 43.).

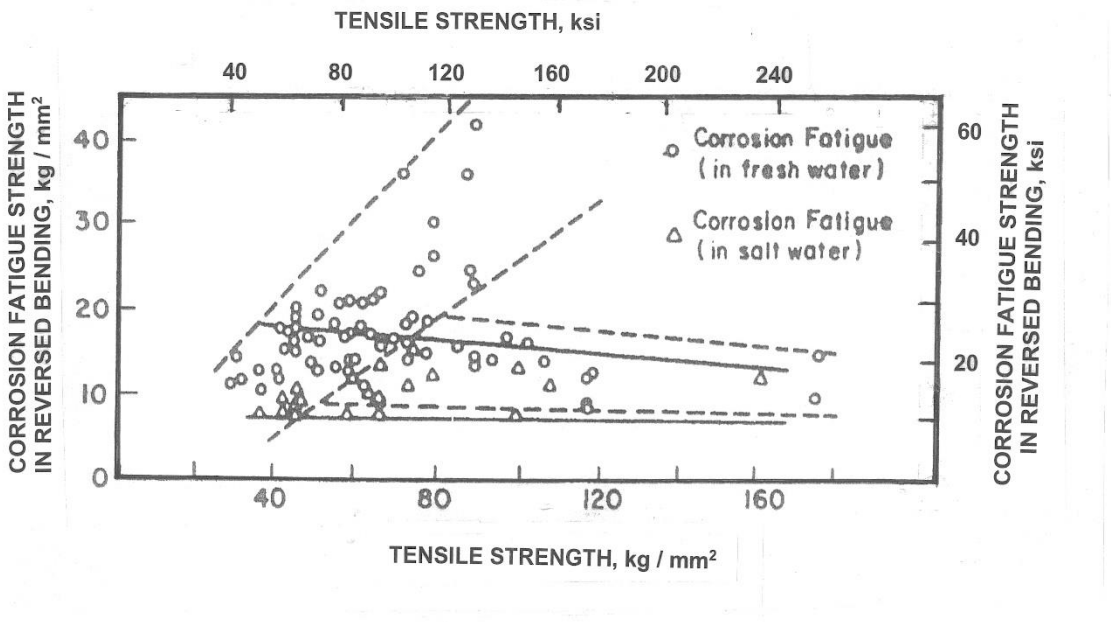

Figure 8. The corrosion fatigue strength of structural and alloy steels incrementally decreases with increasing tensile strength, especially in saline waters, unlike their performance in dry air where fatigue strength is directly proportional to tensile strength.

Typically, smooth specimens in rotating bending in dry air have a fatigue / tensile strength ratio of 0.50 to 0.55 at a strength range of 60 to 200 ksi. In saline water in continuous immersion, that ratio sharply decreases to 0.10 to 0.20.

The empirical equation for corrosion fatigue strength vs. tensile strength for the above plot in *Figure 8* is $\sigma_{\text{corr-fatigue}} = 0.0315\ (\text{UTS}) + 11.2$, where UTS is in ksi. Fatigue strengths in this graph are for continuous immersion in salt water at 10^7 cycles, which would apply to conditions of long-term exposure to very frequent deicing, or continuous salt fall or ocean spray in coastal locations.

Pits rapidly form in carbon and alloy steels when exposed to chlorides within the first years of exposure [Ref. 19, F. Fink and W. Boyd, *Corrosion of Metals in Marine Environments*, Defense Metals Information Center Report 245, Columbus, May 1970, p 12.). Without protection from depleted zinc, the pit depth rates created in steels subject to chlorides are about 2.3 that of uniform weight loss of steel as expressed in mils/yr. The double notch breakaway coupling

microstructure consisted of bainite, acicular ferrite and pearlite. When SAE 4140 is annealed or air-cooled and no martensite is present, the microstructure of these steels is ferritic-pearlitic. Fatigue strength of SAE 4140 as a function of tensile strength is plotted in *Figure 6.* As the tensile strengths of SAE 4130, 4140 and 4340 steels increase, their sensitivity and the reduction of fatigue strength also increases when exposed to certain environmental effects. These effects include exposure to moisture, chloride salts and aeration and result in reduction of fatigue life compared to the same stress in dry air or inert argon gas. Corrosion fatigue crack growth rates increase as the stress cycle frequency decreases [Ref. 21], as shown in *Figure 9 (from Science Direct Topics—Corrosion Fatigue, p 12, extract from B. Popov, Corrosion Engineering, 2015)*.

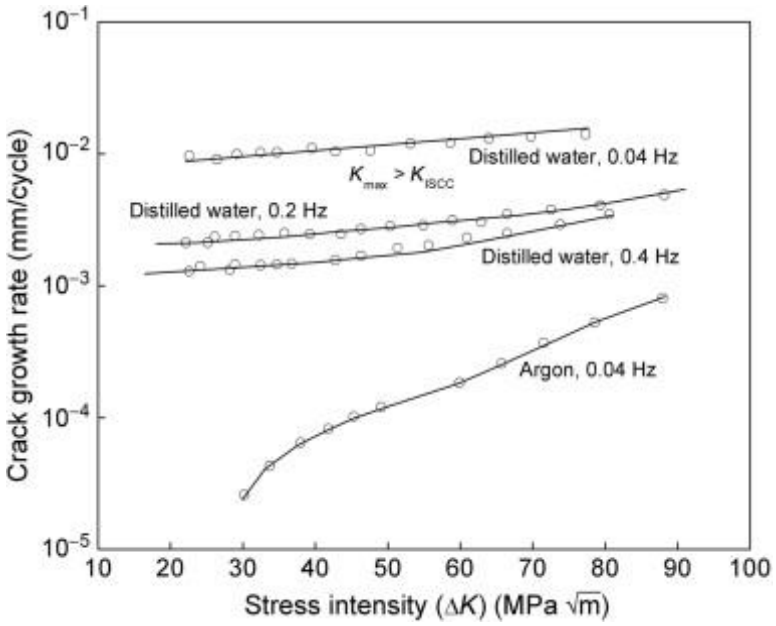

Figure 9. Compared to an inert atmosphere of argon, the crack growth rate for higher tensile alloy steels (SAE 4340 shown in this graph) increases in the presence of moisture and if the cyclic rate of stress application decreases.

Crack propagation rates were taken from research work performed by the Naval Research Laboratory for steel fatigued at low cyclic frequencies in air and saline media, as shown in *Figure 10*. The corrosion rate of steel increases in moist environments where chlorides are present. For very warm locations, the corrosion rate of steel is 5.8 mpy where there is salt accumulation and dust was present (couplings are at ground level), whereas in colder areas it

decreases to about 1.1 mpy [Ref. 22, S. Coburn, “Atmospheric Corrosion”, Metals Handbook, Vol. 1, Properties and Selection: Irons and Steels, ASM International, Metals Park OH, 1978, p. 720. A composite corrosion rate of 3.5 mpy for the SAE 4140 steel was determined to be reasonable, with pit rates at about 2.3 times that of the overall corrosion rate.

In the case of the coupling, once the 1.5 mil eta layer of zinc is consumed in about 7 months, whereby the more brittle zinc-iron layers are then subject to cracking. Using a pitting depth rate of 7 mpy for the 4140 steel coupling, pit depth leading to cracking would have advanced to about 0.014” after about 2 years, with higher corrosion rates in the spring and summer months where they increase by 0.532 for each °C [Ref. 24, R. Melchers, Corrosion of Structural Steel Immersed in Seawater, J. of Infrastructure Systems, Vol. 12, Issue 3, Sept. 2006, Fig.2] and when wetted with dew that creates a saline solution with deicing fluids [Ref. 20, F. Fink and W. Boyd, The Corrosion of Metals in Marine Environments, Defense Metals Information Report, Bayer & Co., Columbus OH, 1970, p. 12.

The first major windstorm after penetration of the zinc coating and pit formation occurred in October 1988 at 53 mph, and then another storm occurred in March 1991 when peak wind speeds were 71 mph. Light poles have a typical fundamental frequency of about 1 Hz. Crack growth rates substantially increase compared to much lower crack growth rates obtained at frequencies of 10 Hz. Because of decreased frequency of opening and closing the corrosion fatigue crack, this allows more time for ingress of water and air to further accelerate crack growth.

The crack growth rate for steels with higher tensile strengths is a combination of dry air fatigue, corrosion fatigue and stress-corrosion cracking. Stress corrosion cracking may be a contributor to the corrosion fatigue of the couplings, resulting from the effects of the zinc coating that generate electrons which may not form hydroxyl ions in a tight crack of the 4140 steels, but instead generate hydrogen due to lack of oxygen and localized acidity from deicing salts.

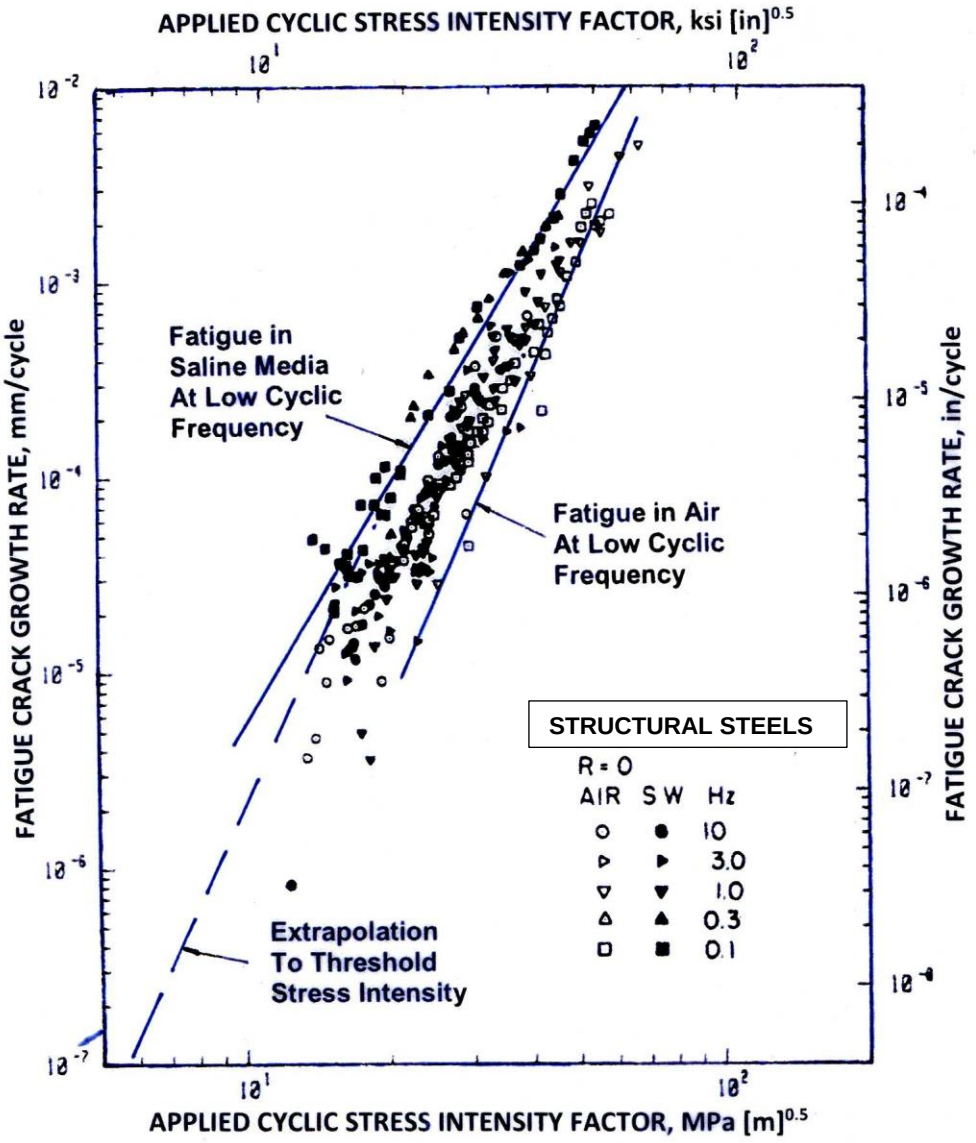

Figure 10. The general fatigue crack growth rate for structural steels increases in saline media at low cyclic frequencies, such as when salt spray is encountered due to application of deicing salts, compared to low cyclic frequencies in air. In general, extrapolation for low frequencies have cracking thresholds at 6 ksi $[in]^{0.5}$ increasing to 9-10 ksi $[in]^{0.5}$ at 1 Hz. Source: [Ref. 23, *Naval Research Laboratory Memorandum Report 4467*].

However, since the tensile strength of the coupling is about 125 ksi, it is less susceptible to stress-corrosion cracking than other steels that have tensile strengths of 150 ksi or more. Applying the zinc potential of -0.763 vs. standard hydrogen electrode does not decrease crack propagation rates. At cyclic frequencies less than 1 Hz, crack propagation rates can increase substantially. If the pole has a cyclic frequency of less than 1 Hz, application of zinc coatings may increase crack propagation rates [Ref. 19]. C. Jaske, J. Payer and V. Balint, Corrosion Fatigue of Metals in Marine Environments, Metals and Ceramic Information Center, MCIC Report 81-42,Columbus, OH, July 1981, p 64.

For uncoated SAE 4140 steel in moist environments or immersed in saline solutions, the time to initiate cracking has been investigated at various yield strengths. The crack initiation threshold in benign environments was found to be a function of the notch root radius and ΔK total and directly related to the yield strength of the alloy. The crack initiation threshold was found to be independent of the stress ratio [Ref. 8, p. 267]. This relationship was determined to be:

$$\Delta K_{total} \div [\rho]^{0.5} = 10\,[\sigma_{ys}]^{0.5}$$

Where

ΔK_{total} = stress range, ksi

ρ = notch root radius

σ_{ys} = yield strength, ksi

Substituting the values for root radius of 0.0625” and 98.7 ksi yield strength for the double notch coupling, ΔK = 24.8 ksi $[in]^{0.5}$. This value is substantially greater than the threshold for corrosion fatigue cracking obtained by the Naval Research Laboratory shown in *Figure 9.* If this value is associated only with deflection by wind forces, the Navy data shows that the threshold stress is approximately 10 ksi $[in]^{0.5}$. For a crack length of about 0.010, this is a coupling stress of 51 ksi, equivalent to a windspeed at 50 mph, a common wind occurrence in Illinois.

The number of cycles to initiate a crack to begin corrosion crack growth is based on the previous equation where the yield strength $10\,[\sigma_{ys}]^{0.5}$ is substituted for $\Delta K_{total} \div [\rho]^{0.5}$. The corrosion crack initiation equation is $N = 3.56 \times 10^{-11} \times (\Delta K_{total} \div [\rho]^{0.5})^{-3.36}$. Since the value of $10\,[\sigma_{ys}]^{0.5} = 10\,[98.7]^{0.5} = 99.3$, when it is inserted into the corrosion crack initiation equation, then $N = 99^{-3.36} \times 3.56 \times 10^{11} = 69{,}455$ cycles. This stress level of 99.3 ksi is virtually equivalent to the predicted yield strength of 98.7 ksi of the SAE 4140 coupling. The total number of hours required to start a corrosion crack, based on 3600 secs in one hour and a fundamental

frequency of 1 Hz for the light pole, would be 69,455 ÷ 3600 = 19.3 hours for the SAE 4140 steel coupling. A high-speed wind event above 50 mph, typically lasts no more than one hour.

Based on construction records, the poles were installed in between 1987-1988. Since the failure occurred in 2016, the poles were about 28-29 years of age. Over a 29-year period, there were numerous occasions when wind speeds exceeded 50 mph. Stress intensities gradually increase when crack lengths increase due to corrosion fatigue and pitting. Crack growth rates that were present at crack initiation at higher wind speeds can be sustained at lower wind speeds after crack growth had resulted in generating cracks of greater depth. This is because crack growth is function of stress intensity, which is the product of stress concentration and crack length when an edge crack is involved.

Several mechanisms to create pits and initiation cracks were operating, causing the couplings to be susceptible to failure. The loss of galvanized pure eta zinc due to atmospheric corrosion eventually reaches the more brittle delta and gamma zinc layers which aid in the formation of shallow cracks. Zinc alloys with greater iron content, particularly the delta and gamma phases, provide lesser galvanic protection. Further penetration into the SAE 4140 base metal by these zinc-iron galvanizing alloys may have resulted in minor effects of hydrogen embrittlement if deicing chlorides are present. Shallow pits can open-up due to tensile stresses resulting from wind-induced forces acting on the light poles.

All three mechanisms that contribute to corrosion fatigue of higher strength steels could have been potentially operating, depending on prevailing conditions. They include (1) brittle zinc-iron phases from galvanizing that form micro-crack initiation sites; (2) pitting due to chlorides from sprayed deicing fluids and surface imperfections; and (3) sensitivity of higher yield and tensile strength alloys to hydrogen embrittlement.

The minimal fracture toughness of 25 ksi $[in]^{0.5}$ of the SAE 4140 coupling steel is another contributor to premature failure, decreasing the critical crack depth. At 40 mph, the critical crack depth was determined to be 0.191".

8. *Crack advancement*. Once initial cracks form due to zinc and corrosion fatigue, crack

advancement in alloys like SAE 4140 will increase in comparison to crack propagation in air. The crack advancement rate of da/dN for ferritic-pearlitic steels in air and in saline media has been previously determined by the Naval Research Laboratory, as shown in *Figure 9*.

It was estimated that the steel light poles, after being forced in one direction by winds, would elastically oscillate at the same tensile position within the fundamental frequency of 1 Hz and experience periodic tensile stresses as long as higher wind velocities continued. Wind velocities above 50 mph were considered. Wind velocities of 70-80 mph are relatively rare occurrences in Illinois. Gusting winds often have a frequency of 1 Hz, leading to vibration of the pole at its fundamental frequency of the light pole which is also 1 Hz [Ref. 25]. reference to Blackmon, Weber and Chiswell, 2015).

Cracks were found in the fracture surfaces of the coupling that ranged in depth from 0.020" to 0.191", depending on where crack initiation and eventual failure took place. The variation of the crack depth and position occurs because wind directions are also variable, resulting in wind loadings causing crack initiation around the entire periphery of the breakaway notch. The zinc coating consists of a relatively pure eta zinc layer which is about 50% of the coating thickness. The remainder of the zinc coating is a combination of Zn-Fe alloys that are more brittle in nature. In other double notch couplings which have failed, numerous peripheral cracks were found, whose typical depth was about 0.040-0.075". Crack propagation rates, based on occurrence of the highest wind speed events since 1987, were computed at an average initial crack depth of 0.015" for the failed coupling in *Table 5* for illustration purposes.

The stress intensity for crack propagation was computed as $K = 1.1\ \sigma \times [\pi\ a]^{0.5}$, where a is the crack depth. See *Figure 10* for the stress intensity compliance K_I for a plate with a side crack in tension. Crack advancement was determined by the highest wind speeds sustained in the Springfield area from 1987 to 2016. This was accomplished to give an indication of how crack advancement led to a critical crack depth when the pole failed during an extended windstorm on October 17, 2016.

As a crack advances, stress intensity increases. At 39 mph, the nominal notch coupling stress is 13.1 ksi, but the nominal stress is concentrated to 32.4 ksi because of the V-shaped deep notch of the coupling. Stress intensity K_I at a crack depth of 0.075" is $1.1\ (32.4)\ [\pi \times 0.075]^{0.5}$,

which equals 17.3 ksi $[in]^{0.5}$, whereas at a crack depth of 0.190", K_I is 27.5 ksi $[in]^{0.5}$, which is nearly 60% greater intensity than at 0.075" depth.

Springfield sustained five high speed wind events after the couplings were installed. These wind events are summarized in *Table 7*, along with their corresponding coupling stress levels as calculated by the empirical equation derived from *Figure 5*.

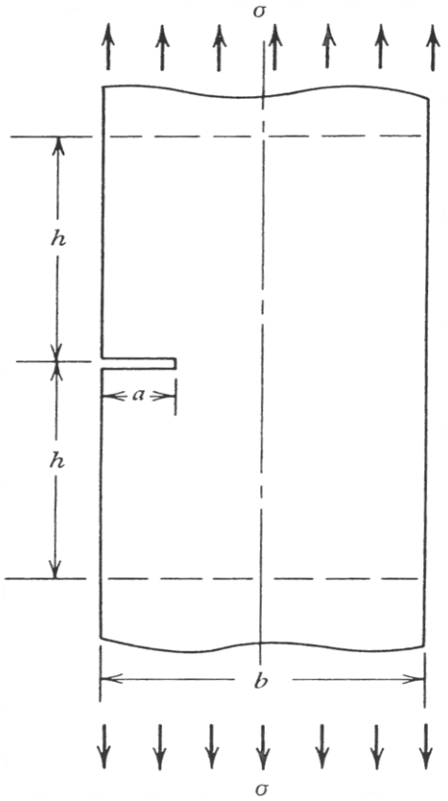

Figure 11. The compliance K_I for a side-cracked element is $K_I = C\ \sigma\ [\pi a]^{0.5}$ where C = 1.1 for shallow cracks and σ is either nominal or concentrated stress, which determines the stress intensity of a crack based on its length. This compliance was selected because the fracture surfaces of the couplings indicated cracks starting from one side of the notch, rather than uniform depth cracking around the periphery of the notch.

***Table 7 /* Major Wind Speed Events Since 1987**

Date of Event	*Wind Direction*	*Sustained Wind Speed, mph*	*Nominal Notch Stress, psi* [A]	*Concentrated Notch Stress, psi*
October 17, 1988	Southwest	53	12,589	39,026
March 27, 1991	Southwest	71	20,550	63,705
April 19, 2002	Northeast	74	22,001	68,203
May 30, 2008	West	68	19,134	59,315
February 2014	Southwest	64	17,302	53,636
October 2016	South	38 [B]	6,930	21,483

[A] Nominal section stress stated in the table does not include loss of section due to crack advancement.
[B] Average stress over 3 hours duration.

Crack advancement rates were started from an average crack depth of 0.015". Sustained winds were estimated to have a duration of no more than one hour. Since the fundamental frequency of the poles is 1 Hz, a total of 3600 secs was accorded to each series of crack advancements. Since the coupling is composed of a steel with a pearlitic-ferritic microstructure, the crack advancement was determined from *Figure 12* starting from an initial crack depth of 0.014". This initial crack is determined for loss of 0.002" of zinc and steel pit depths of 0.012 after two years of exposure to deicing salts. Since crack shapes were shallow, the concentrated notch stresses generated by specific wind speeds were used. Progressive crack advancements are summarized in *Table 8.*

After 29 continuous years applications of wind less than 50 mph, and based on crack growth from major storms, the final crack depths of all four couplings ranged from 0.079" to 0.191".

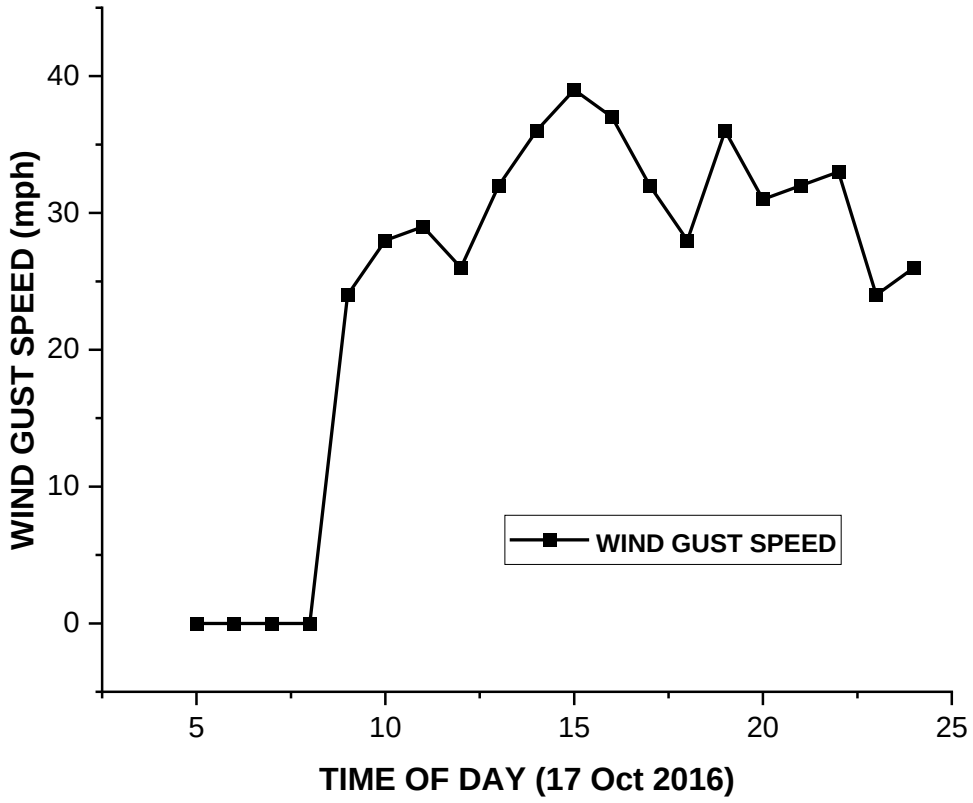

Figure 12. On the day when the couplings failed, Springfield experienced a windstorm that lasted 16 hours. The strongest winds began at 1:00 pm to 9:00 pm, whereby the average wind speed was 25.4 ± 4.4 mph and average wind gust was 33.7 ± 3.5 mph, yielding a gust factor of 1.33. Peak winds were 37, 39 to 38 mph over a 3-hour period, for an average of 38 mph. The gust factor of 1.33 is commonly used in other wind speed calculations to approximate wind pressure fluctuations, which increase as a function of height. Data source: *National Weather Service of NOAA for Lincoln Capitol Airport,* which is approximately 2.4 miles distant from the pole location.

***Table 8 /* Progressive Crack Advancement Generated by Major Wind Events**

Wind Speed, mph	*Notch Stress, ksi*	*Stress Intensity Change (ΔK)*	*Crack Propagation Rate, in/cycle*	*Crack Advancement in 3600 secs, inches*
53	39.0	39.1 (1.1) $[\pi \times 0.014]^{0.5} = 9.0$	3×10^{-7}	0.001
71	63.7	63.8 (1.1) $[\pi \times 0.015]^{0.5} =$ 15.2	2×10^{-6}	0.007
74	68.2	68.3 (1.1) $[\pi \times 0.022]^{0.5} =$ 19.7	8×10^{-6}	0.029
68	59.3	59.4 (1.1) $[\pi \times 0.051]^{0.5} =$ 26.1	1.3×10^{-5}	0.047
64	53.6	53.7 (1.1) $[\pi \times 0.098]^{0.5} =$ 32.7	2×10^{-5}	0.072
38*	21.5*	21.5 (1.1) $[\pi \times 0.170]^{0.5} =$ 17.2	2×10^{-6}	0.022*
Total	…	…	…	0.192*

*Based on an average of wind gusts and crack advancement over 3 hours (10800 secs) on 17 October 2016. The measured coupling critical crack depth of 0.191" deviates from the predicted crack depth 0.192" by only 1%.

Based on this simplified analysis, the estimated crack propagation during the time of fracture was 0.022" over a period of about 3 hours. At 37-39 mph, a concentrated average stress of 21.5 ksi was generated in the notch. Depending on whether the notch contained substantial chloride content, crack propagation rate could have varied between 1×10^{-6} to 3×10^{-6} in per cycle.

In either case, the windstorm was of such a long duration whereby either crack propagation rate would have caused two couplings to fail, causing rapid load transfer to the remaining couplings. Metallographic measurements show that the actual critical crack depth was 0.191". The peak wind on 17 October was near 40 mph, generating a calculated concentrated stress of 22,000 psi which assumes a gust factor of 1.14, although the average gust factor was 1.33. If a 1.33 gust factor is used, this increases the concentrated stress to 25.7 ksi. This results in a stress intensity of (25.7) (1.1) $[\pi (0.191)]^{0.5} = 21.9$ ksi $[in]^{0.5}$. This value is within 11% of the predicted fracture toughness of 24.5 ksi $[in]^{0.5}$ of the coupling body based on the CVN impact energy

absorption of 5 ft-lbs correlated by the Barsom-Rolfe equation. The difference between the calculated depth of 0.192” based only on crack advancement from major windstorms vs. actual 0.191” measured crack depth is only 1%.

There is a direct correlation of CVN to K_{Id} fracture toughness and critical crack depth. The actual crack propagation depth was also very well correlated to major wind events. Couplings failed at the lesser wind speed when stress levels and crack depths were within those predicted by CVN to fracture toughness correlations of 24.5 ksi $[in]^{0.5}$. This is a direct confirmation that coupling failures were due to their very low fracture toughness, their intentional notch sensitivity associated with the coupling design, decreased high cycle fatigue strength due to galvanizing, and exposure to substantial windstorm events over a 28-year period of service that affected their durability after installation.

Figure 13. The initial crack surface shown here as the darker thumbnail-shaped area between the 2:00 to 4:30 position of the notched section. The coupling notch crack has a measured depth of 0.191”.

Figure 14. The other coupling with a prominent fatigue crack at the 6:00 to 11:00 position, with a shear lip at the 2:30 to 6:00 position. The initiation crack has a somewhat irregular shape, with the deepest penetration of 0.190” at the 10:30 position.

Figure 15. The third coupling has incipient initial fatigue cracks at the 8:00 to 10:30 clock position but exhibits relatively faster crack propagation fracture surfaces as loads were

transferred from the other two couplings that had sustained deeper cracking. Crack depth varies from 0.051” to 0.104”.

Figure 16. The fourth coupling, showing initial fatigue cracking at the 8:30 to 11:30 position at a depth of 0.171", leading to a fast-fracture river gorge-like pattern beginning at 12:00, shows divergence into a shear failure deep valley and peak of almost 70% of its ruptured section.

Mechanism of Failure

1. *Installation.* A contractor installs the breakaway couplings by tightening the nuts onto the threaded extension. Depending on the amount of torque, this induces a prestress level into the coupling which is attached to an anchor bolt. Some of this prestress is decreased by the weight of the light pole, which typically does not exceed 1,000 lbs. According to double notch coupling installation instructions, the top nuts are to be tightened by 1/3 turn after being torqued to "snug tight". Assuming "snug tight" induces no more 0.005" of deformation, a 1/3 turn on a 1"-8 UNC thread results in 0.045" of deformation. The length of the coupling undergoing deformation is 240 mm (9.449"), which results in a strain of approximately 0.050 ÷ 9.449 = 0.00529 strain. Since the modulus of elasticity of steel is 30 x 10^6 psi, the nominal stress induced would be 158,750. This value is unrealistic because it assumes a perfect fit and alignment and parallelism of washers, pole base, coupling and nut faces. If the compression of the washers, pole base and lack of parallelism would decrease the actual amount of axial deformation to only 0.015" as "snug tight", the strain induced is 0.015 ÷ 9.449 = 0.00159 in/in. The preload on the coupling would be a nominal 47,700 psi, which is still a substantial portion of the elastic range of the coupling. This does not consider any stress concentration effects associated with the coupling notches. The required 1/3 turn-of-the-nut torque after being "snug tight" partially contributed to fatigue and safety issues because of the establishment of a mean stress in the coupling notch. To induce a "snug-tight" stress of 5 ksi into the notch, only 25 ft-lbs torque is required when using machine oil or thread locker paste as a thread lubricant.

When mean stresses were applied to SAE 4140 and 41L40 that were fatigued in saline water, their number of cycles to failure decreased, with only minor differences when the 4140 tensile strength was increased from 216 ksi to 236 ksi. Loss of high cycle fatigue life at 40 ksi mean stress vs.60 ksi mean stress was about 75% [Ref. 26], D. Tipton, Corrosion Fatigue of High

Strength Fasteners Materials in Seawater, DOE/NASA Report CR-174677, Wash DC, Dec 83, pp 8-10. This loss of fatigue life is shown in *Figure 17*.

The weight of the pole decreases the stress levels in the notched areas. If the pole weighs 1,000 lbs, and this weight is equally distributed among the four couplings, each notched area receives 250 lbs of compressive force. The notched area is 0.358 in^2. With the application of 250 lbs per notch, this is a compressive stress of approximately 700 psi, which provides only minor relief from the preload stresses resulting from the 1/3 turn-of-the-nut.

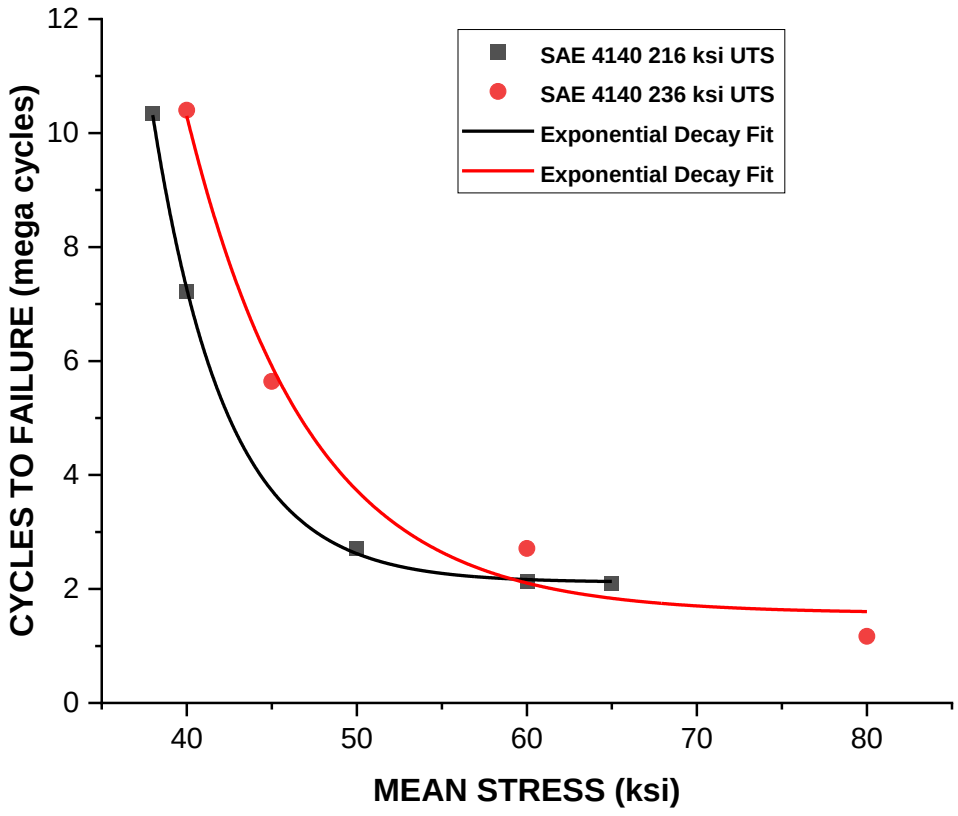

Figure 17. A mean stress is imposed on the coupling notch due to excess tightening of the coupling nut when both “snug tightness” and “1/3 turn-of-the-nut” are both used to fasten the coupling to the anchor bolts and pole base. Mean stress has adverse fatigue effects on

couplings in all environments, including dry air, higher relative humidity, and is most severe under saline conditions resulting from exposure to deicing fluids or coastal salt fall.

2. *Galvanizing and corrosion fatigue.* The manufacturer recommended 2/3 turn-of-the-nut after a “snug-fit” of the nut. Although the coupling failed after 28 years, it was able to withstand a peak wind gust of 74 mph. That generated a nominal stress of 22 ksi in the couplings. The fatigue strength of the coupling, after galvanizing a. The 1/3 turn-of-the-nut torque induces a mean stress. It is possible that vibration could have decreased this preload value based on its time of service. No thread locking compounds were used or recommended for the nuts by the manufacturer.

The Goodman fatigue equation is a widely used relationship to determine whether metal failure will occur:

$$(S_a / S_f) + (S_m / S_u) = 1$$

Where
S_a = nominal alternating stress, 21 ksi at 71 mph
S_f = fatigue strength, with K_t = 3.1 notch, 39 ksi at 10^5 cycles
S_m = mean stress (to be determined by calculation)
S_u = ultimate tensile strength, 123 ksi

To determine the mean stress that would cause failure, $S_m = [1 – (S_a / S_f)] \times S_u$. Substituting in the various values, the mean stress $S_m = (1 – 0.56) \times 123 = 54$ ksi. This indicates that an estimated preload stress resulting from tightening the coupling according to the manufacturer’s installation instructions could cause fatigue damage, especially after the coupling had been exposed to conditions of salt spray after 28 years. For the couplings to survive their first major windstorm, the mean stress had to be less than 54 ksi. If it is assumed that the manufacturer’s requirement of 1/3 turn-of-the-nut was followed, a reduction of mean stress less than 54 ksi probably resulted from a gradual loss of a rigid connection after years of service, or the 1/3 turn-

of-the nut procedure was not followed at installation. However, a mean stress of 54 ksi would exceed the low corrosion fatigue strength of about 15 ksi at 10^7 cycles. Reducing the mean stress due to application of 1/3 turn-of-the-nut can be alleviated by use of thread locking compounds (such as Loctite 242 or 262), and then applying a limited amount of torque to tighten the nut (25 ft-lbs induces only 5 ksi in the notch).

3. *Fatigue life and load transfer.* When the fatigue lives of the first and second couplings were nearly consumed, this resulted in more crack initiation and propagation in the other two couplings. When the crack lengths in the first two couplings were in critical range, causing the first and then the second coupling to fail. Such a substantial load and stress transfer that occurs at the speed of sound in metals, rapid failure occurs. The fracture toughness of the couplings was severely limited in the first place. The CVN tests indicated that only 5-6 ft-lbs of energy absorption was available at normal temperatures. These low impact energy values translate to a K_{Id} fracture toughness range of only 24 to 27 ksi $[in]^{0.5}$.

Since there are normally four couplings and two notches per coupling, there are 8 total notches at the base of the pole. Two notches per couplings further increases the probability of crack formation. The failure of the first coupling reduced the load-carrying capacity of the remaining couplings by 25%. At 29.3 ksi of concentrated stress at 37 mph and a fracture toughness of 24.5 ksi $[in]^{0.5}$, the critical crack depth is 0.278", but if increased to 36.6 ksi in the second coupling, critical crack depth decreases to only 0.118". It appears that two couplings had already sustained cracking of substantial depths. Due to its limited ability to carry this transferred load, the second coupling also failed, resulting in more rapid cracking and then fast fracture rupture of the two remaining couplings. This procession of load transfers to remaining couplings that were largely intact thereby caused the light pole to fall onto Veterans Parkway.

Conclusions and Recommendations

The alloy steel double notch breakaway couplings failed due to a combination of the following factors:

1. Reduction of the fatigue strength of SAE 4140 due to galvanizing.
2. Corrosion of the zinc coatings and base metal due to atmospheric and salt spray effects from highway deicing salts.
3. Very low impact and fracture toughness of the couplings, resulting in reductions of critical crack lengths, leading to premature failure.
4. The material heat treat parameters of these breakaway couplings are not known, nor is the required galvanized coating thickness correct, because the ASTM standard cited by the manufacturer is for sheet materials and is not intended for components like couplings. The appropriate standard is ASTM A123.
5. The presence of two notches on a single coupling doubles the likelihood of failure. Replacement designs should have only one rupture section. Other impact failures of double notch couplings have left stubs that are not permissible per AASHTO standards after the couplings ruptured, because they could cause fuel tank penetration to the colliding vehicle.
6. Tightening by the “1/3 turn-of-the nut” method results in a higher mean stress on the couplings, reducing their fatigue lives. Instead of turn-of-the-nut, thread locking compounds should be applied to threads and the amount of “snug-tightness” torque should be reduced to a minimum. Apply a “snug-tight” torque of 25 ft-lbs only induces 5 ksi in the coupling notches.
7. The impact toughness for the couplings was very low at 5-6 ft-lbs. Because impact energy absorption is directly related to fracture toughness, critical crack depths at various stress levels are also reduced. If fracture toughness of the couplings is increased by use of a different material or changing the thermal processing of the SAE 4140 presently in use, it is uncertain how this will affect the rupture characteristics of the pole base couplings when they are

impacted by vehicle collision and the resulting deceleration. This will have to be determined by additional testing by an independent testing laboratory conducted on behalf of the coupling manufacturer.

8. Because of the zinc oxide formation, it was difficult to determine whether the couplings had sustained any cracking by simple visual inspection. No obvious rust bleed-out was observed. This makes it more difficult for inspectors to determine if failure is imminent, or if couplings need to be replaced.

9. It is evident that the designers of the couplings clearly intended to achieve frangibility upon impact of poles by vehicles but did not select the correct alloys for couplings that could be exposed to saline media, and they had inherently low impact low toughness. The fatigue strength of higher yield steel alloys like SAE 4140 is markedly decreased in saline media, which easily forms from deicing salts or from salt fall near ocean coastal locations when dew forms moisture and because salt is hygroscopic. The zinc coating is readily consumed under these conditions and provides minimal life extension, and further degrades fatigue strength by liquid metal embrittlement.

10. Maintenance crews stated that there were no scrapes or impact dents on the pole were present after it had collapsed. This indicates that damage was entirely caused by cumulative effects of preload, wind force loadings and inherent pole vibration over a 28–29-year life. Fundamental frequency of the pole was determined to be 1 Hz. However, the breakaway couplings should not have failed at 40 mph because they were rated to withstand windstorms of at least 70 mph of limited duration in accordance with the AASHTO standards for breakaway couplings at the time of their acceptance and installation. Because of the variability of wind speeds in Illinois (or for any other state for that matter), a cumulative damage assessment needs to be done before replacement is required. The use of galvanizing for coupling protection is questionable considering that it degrades the fatigue life of steels. Choice of other alloys with a more appropriate balance of fatigue and corrosion resistance, or use of inert durable coatings, should be considered as alternatives.

11. A realistic life cycle for double notch couplings or any other breakaway designs must be determined by the manufacturer so a practical schedule of replacement of these couplings can be adopted. However, for light poles which have failed, the cost of replacing couplings should ideally be pro-rated based on a specific guarantee of life in years from the manufacturer. This is problematic for couplings that have no life guarantee. Unfortunately, that is case for thousands of couplings presently in the Illinois inventory, which includes State, municipal, county, and local highway agencies. However, if replacements of failed coupling designs are modified and then

subsequently produced, the manufacturer must provide a fixed guarantee of longevity for a specific number of years, free of failure, for all future supply of couplings. This guarantee of a specific coupling life, of course, assumes that the couplings provided would not sustain any vehicle impact damage or rupture due to a pole collision during the guarantee period.

References

1. Model 4100 Specifications Sheet, Transpo Industries, New Rochelle, NY, January 2014.
2. N. Noda, Y. Takase and K. Monda, "Formulas of Stress Concentration Factors for Round and Flat Bars with Notches", *Transactions on Engineering Sciences*, Vol. 13, WIT Press, 1996, pp. 318-322.
3. R. Peterson, *Stress Concentration Factors,* Wiley, New York, 1979, p. 57.
4. E. Dragoni and D. Castagnetti, "Concentration of Normal Stress in Flat Plates and Round Bars with Periodic Notches, *Journal of Strain Analysis*, Vol. 45, March 2010, pp. 495-503.
5. T. Baumeister, E. Avallone, and T. Baumeister III (editors) *Mark's Standard Handbook for Mechanical Engineers,* 8th Edition, Mc-Graw-Hill, New York, 1978, p. 13-18.
6. E. Oberg, F. Jones, H. Horton, and H. Ryffell, *Machinery's Handbook, 26th Edition*, Industrial Press, New York NY, 2000, p. 476.
7. ASM, *Source Book on Industrial Alloys and Engineering Data,* American Society for Metals International, Metals Park OH, 1978, pp. 38; 125.
8. J. Barsom and S. Rolfe, *Fracture and Fatigue Control in Structures, 2nd Edition*, Prentice-Hall, Englewood Cliffs, NJ, 1987, pp. 78; 267.
9. R. Roberts and C. Newton, "Interpretative Report on Small Scale Test Correlations with K_{Ic} Data", *Welding Research Council Bulletin 265*, New York NY, 1991.
10. *Structural Supports for Highway Signs, Luminaires and Traffic Signals, 6th Edition* AASHTO*,* Washington DC, 2013, Table 3.8.4-1.
11. B. Brown, *Stress Corrosion Cracking in High Strength Steels*, Naval Research Laboratory, Washington DC, pp. 52-53.
12. H. Grover, S. Gordon and L. Jackson, *Fatigue of Metals and Structures*, Dept of the Navy, Jun. 1960, p 305.

13. H. Swanger and H. France, “Effect of Zinc Coatings on the Endurance Properties of Steel”, *Bureau of Standards Journal of Research*, Vol. 9, Apr. 1932, pp 9-25,

14. I. Okafor, R. O’Malley, K. Prayakarao and H. Aglan, “Effect of Galvanized Zinc on Microstructure and Fracture Behavior of Low & Medium Carbon Structural Steels”, *Engineering,* Vol. 5, No. 8, Aug. 2013, pp. 656-666.

15. H. McGannon (editor), *The Making, Shaping and Treating of Steel*, 9th Edition, US Steel, Pittsburgh PA, 1971, p. 1033.

16. M. Vermeersh, W. De Waele, N. Van Caenegem, “Liquid Metal Embrittlement Susceptibility of Galvanized Welded Structures of High Strength Steels”, *Sustainable Construction & Design,* 2011, pp. 442-447).

17. C. Slunder and W. Boyd, *Zinc: Its Corrosion Resistance*, International Lead Zinc Research Organization, New York NY, Aug. 1983, p. 106.

18. Y. Meng, et al, “Initial Formation of Corrosion Products on Pure Zinc in Saline Solution”, *Bioactive Materials,* Vol 4., Dec. 2019, pp 87-96.

19. C. Jaske, J. Payer and V. Balint, *Corrosion Fatigue of Metals in Marine Environments,* Defense Metals Information Center Report MCIC 81-42, Columbus, July 1981, pp 43; 64.

20. F. Fink and W. Boyd, *Corrosion of Metals in Marine Environments*, Defense Metals Information Center Report 245, Bayer & Co., Columbus OH, May 1970, p 12.

21. Science Direct Topics—*"*Corrosion Fatigue*",* extract from B. Popov*, Corrosion Engineering,* 2015, p. 12.

22. S. Coburn, “Atmospheric Corrosion”, *Metals Handbook, Vol. 1, Properties and Selection: Irons and Steels,* ASM International, Metals Park OH, 1978, p. 720.

23. J. Krafft, *NRL Memorandum Report 4467*, Naval Research Laboratory, Washington DC, 1973, p. 23.

24. R. Melchers, “Corrosion of Structural Steel Immersed in Seawater”, *J. of Infrastructure Systems*, Vol. 12, Issue 3, Sept. 2006, Fig. 2.

25. J. Blackmon, A. Weber, and S. Chiswell, “Wind Gust Distribution and Potential Effects on Heliostat Service Life”, www.*Science Direct/Article & Abstract /Elsevier Open Access*, 2015.

26. D. Tipton, *Corrosion Fatigue of High Strength Fasteners Materials in Seawater*, Dept. of Energy / NASA Report CR-174677, Washington DC, December 1983, pp 8-10.

27. H. Lee and H. Uhlig, “Corrosion Fatigue of Type 4140 High Strength Steel”, *Metallurgical Transactions*, Vol. 3, Nov. 1979, pp. 2949-2956.

APPENDIX

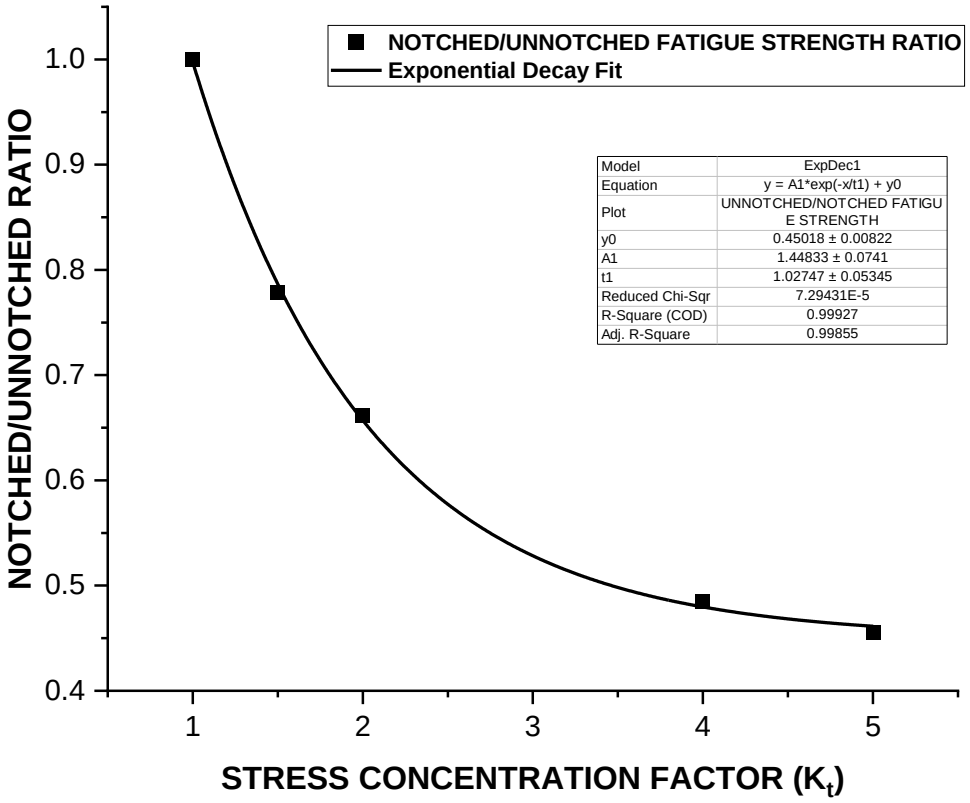

Figure A1. The fatigue ratio of notched / unnotched components substantially decreases as an exponential decay function with notch severity. The predictive equation was derived from fatigue strengths of 0.30-0.40% carbon SAE 4130, 4140 and 4340 alloy steels within the tensile

strength range of 127 to 140 ksi where K_t varied from unnotched $K_t = 1.0$ to $K_t = 5.0$. Data source is [Ref. 12].

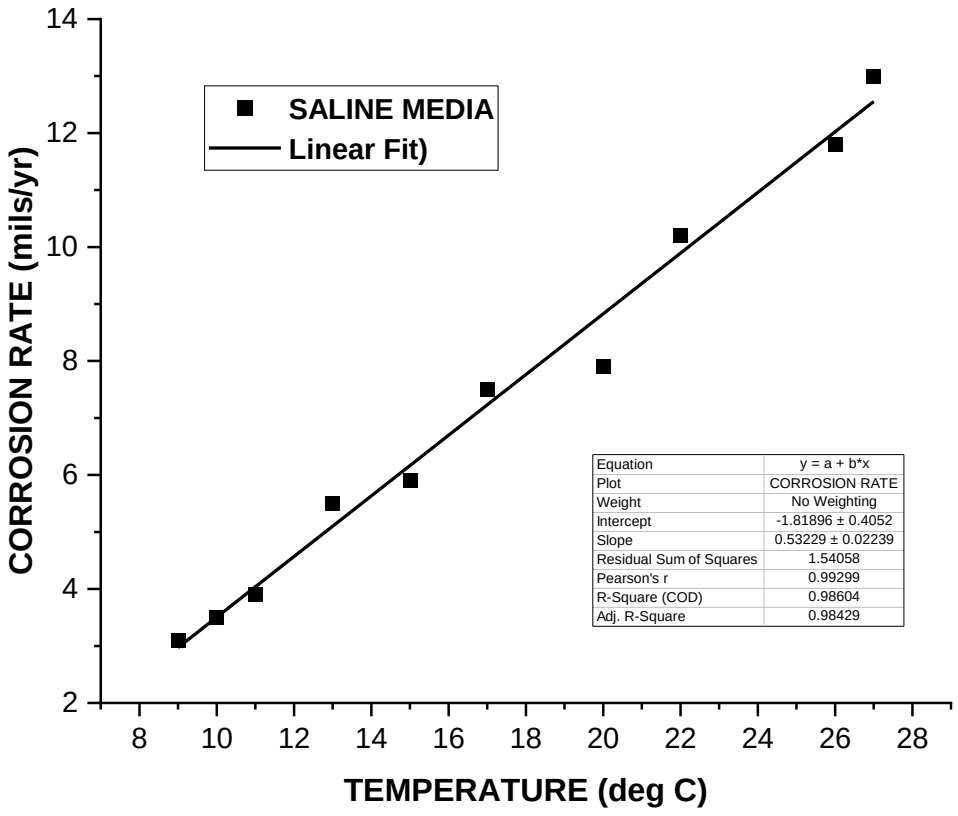

Figure A2. The corrosion rate of structural carbon steels in saline media is a linear function of temperature. The above data was taken from immersion of steels in seawater at different temperatures [Ref. 23]. For other corrosive media, such as in acids or other ionic aqueous solutions, the rate of corrosion may be greater. If passive films are developed on the steel or

alloy, corrosion rates may be less than predicted by rates for carbon steel in waters containing chlorides.

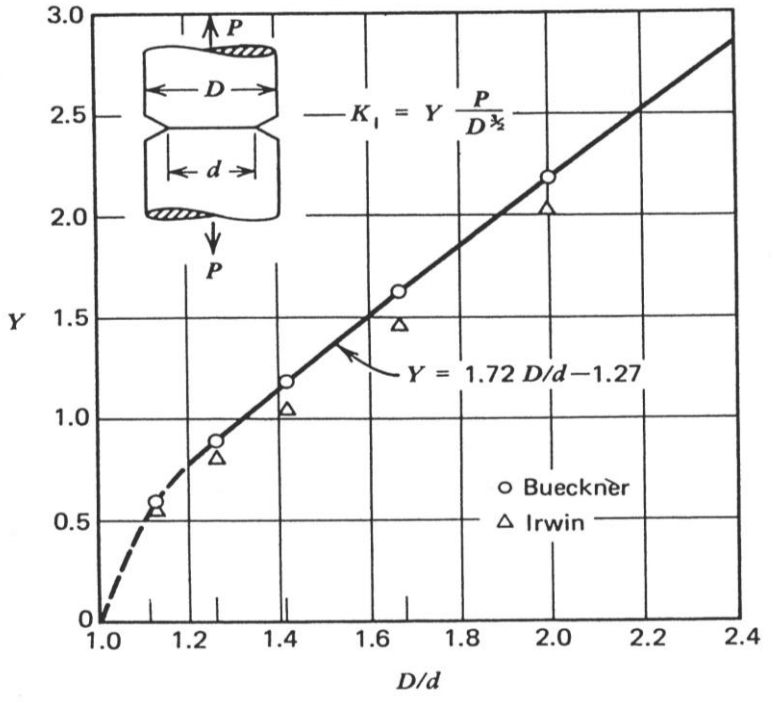

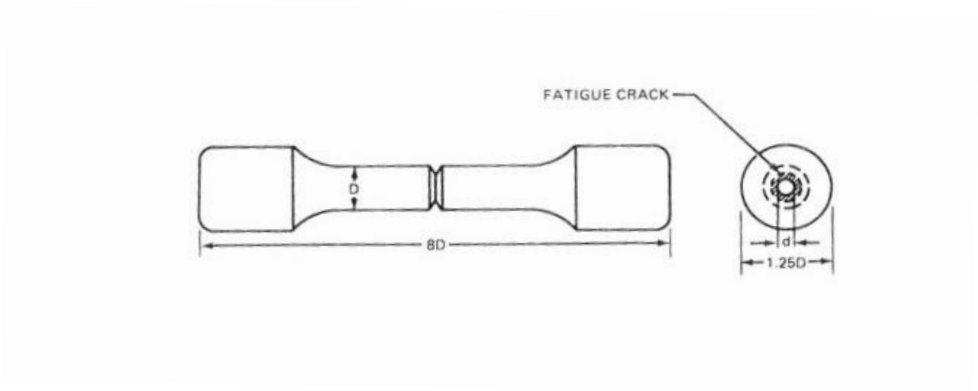

Figure A3. The K_I compliance specimen to determine stress intensity for a centrally notched bar. When the central portion of the notch is cracked, stress intensity can be determined by its circumferential depth. This would apply to a notched coupling where winds frequently change directions to cause a relatively uniform peripheral crack around the notch root. In this report, the cracks were on one side of the coupling, whereby this calibration was not useful. However, this compliance applicable to other couplings in other locations where wind directions are highly variable.

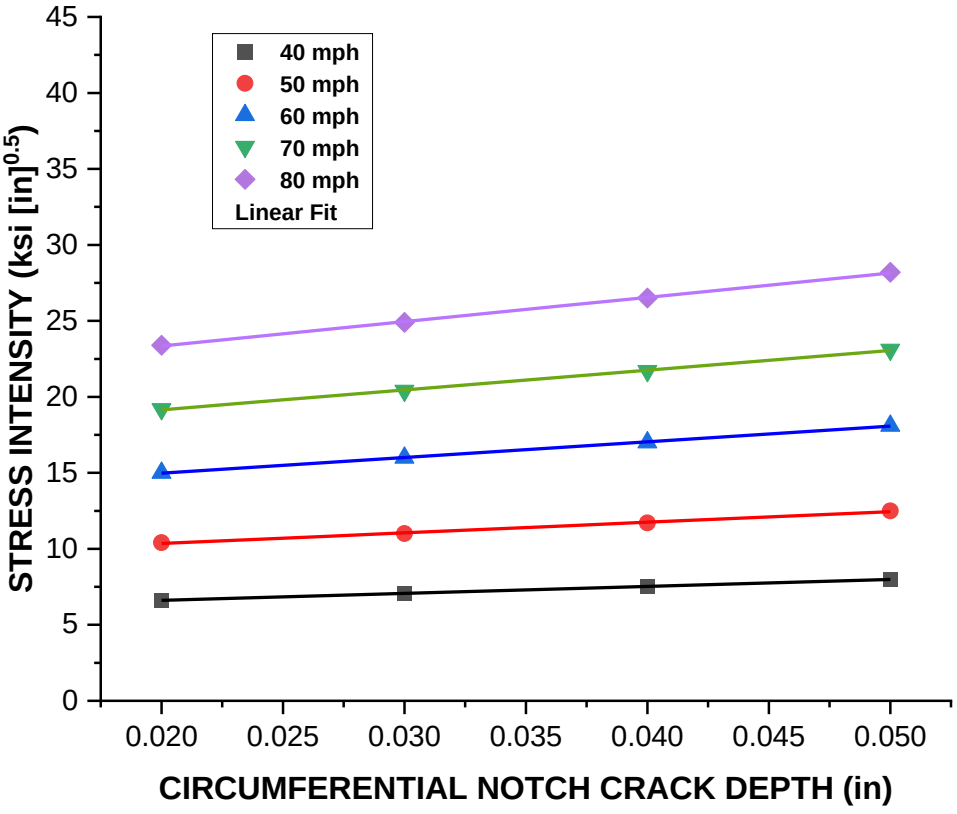

Figure A4. A single notched coupling in the diamond position receives the moment loading when wind forces place it in tension, whereas the opposite coupling is in compression and the side couplings are in the neutral axis. The stress intensity expressed in this graph represents a

case where the crack depth is uniform along the circumference of the notch depth. This would arise if wind directions were changing frequently, causing crack depths to be relatively uniform along the circumference of the notch root. With respect to a coupling with a fracture toughness of 24.5 ksi [in], the critical crack depth would be 0.060" at 70 mph.

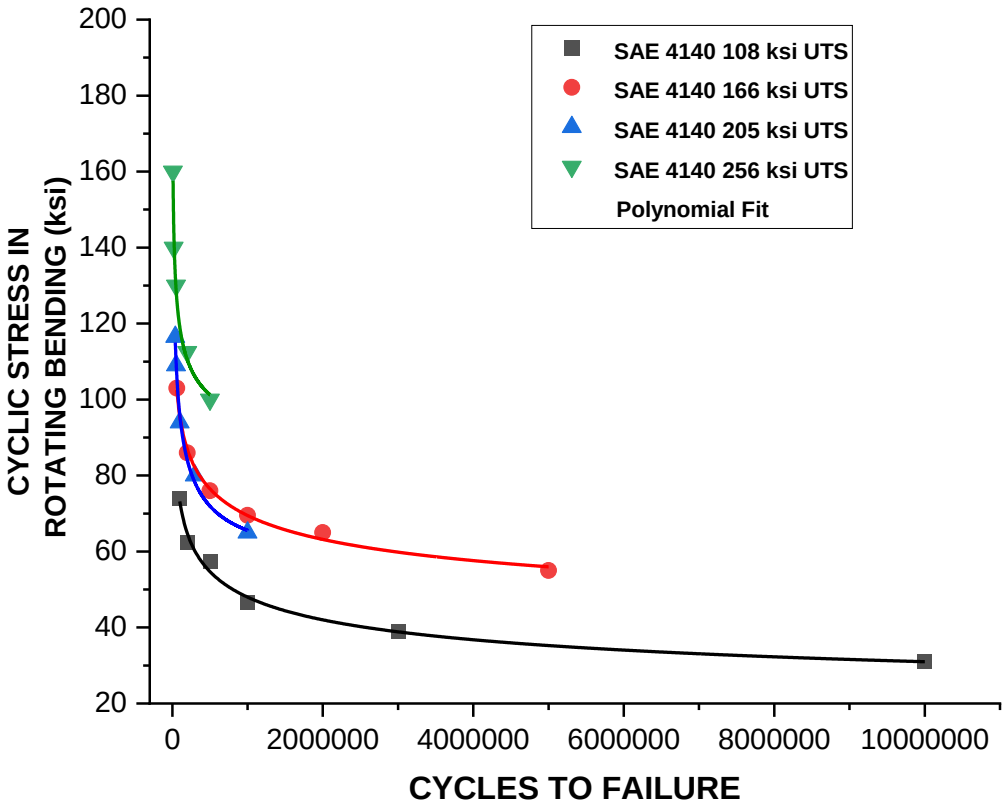

Figure A5. As the tensile strength increases and rotating or axial stresses increase, the number of cycles to failure decreases sharply in saline media. The approximate ratio of 0.5 of fatigue strength / tensile strength at 10^7 cycles is no longer applicable. When the relatively humidity is

elevated above 90%, the proportionality to tensile strength in dry air decreases when UTS is above 165 ksi for SAE 4140. When SAE 4140 is subject to an aerated saline solution, which are analogous conditions for couplings receiving salt spray or salt fall or heavy applications of saline deicing fluids, the number of cycles to failure is markedly reduced if operated at stress levels at 0.5 x UTS. Moreover, the time to failure was found to be directly related to the fracture toughness of SAE 4140, whereby higher fracture toughness values increased the time to failure. Source: [Ref. 27].

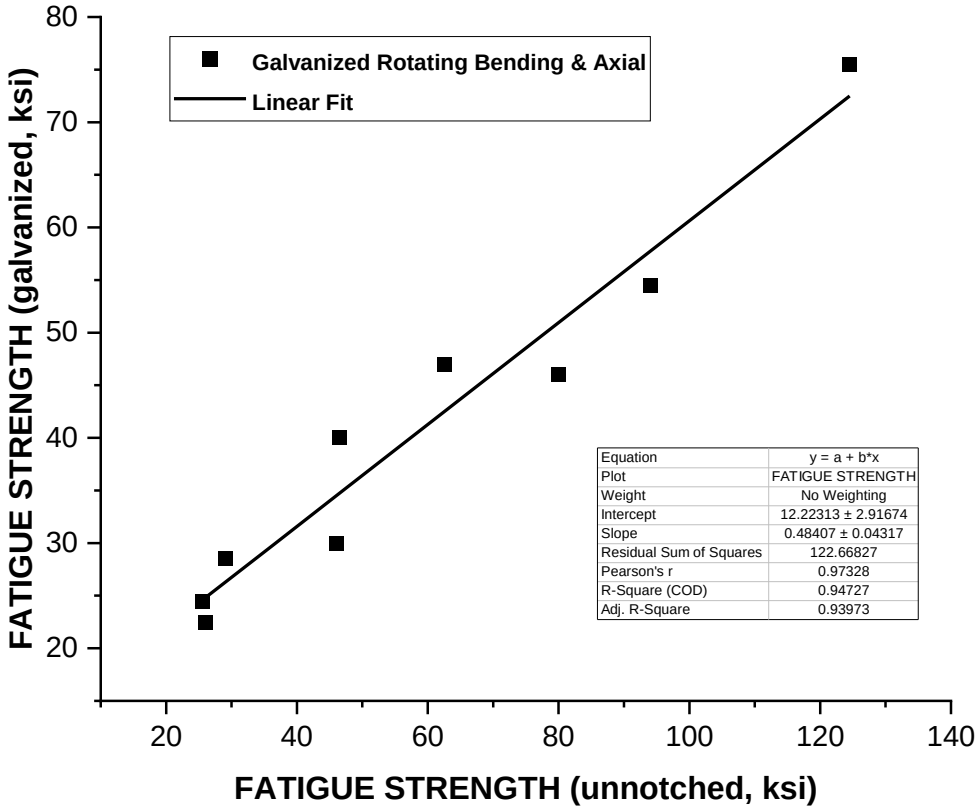

Figure A6. The fatigue strength of an unnotched smooth round bar at 10^7 cycles is reduced by galvanizing in both axial tension and rotating bending. The reduction is a linear function with an inherent error of ± 2.9 ksi. The empirical equation to predict the loss of fatigue strength for carbon steels due to galvanizing is:

$$\sigma_{galv} = 12.2 + 0.484\,[S_f]$$

where:

σ_{galv} = galvanized fatigue strength, ksi

S_f = fatigue strength at 10^7 cycles for an unnotched bar, ksi

NOTES